Click Here for Full Article

Arabia-Somalia plate kinematics, evolution of the Aden-Owen-Carlsberg triple junction, and opening of the Gulf of Aden

Marc Fournier,[1,2,3] Nicolas Chamot-Rooke,[3] Carole Petit,[1,2] Philippe Huchon,[1,2] Ali Al-Kathiri,[4] Laurence Audin,[5] Marie-Odile Beslier,[6] Elia d'Acremont,[1,2] Olivier Fabbri,[7] Jean-Marc Fleury,[8] Khaled Khanbari,[9] Claude Lepvrier,[1,2] Sylvie Leroy,[1,2] Bertrand Maillot,[10] and Serge Merkouriev[11]

[1] New geophysical data collected at the Aden-Owen-Carlsberg (AOC) triple junction between the Arabia, India, and Somalia plates are combined with all available magnetic data across the Gulf of Aden to determine the detailed Arabia-Somalia plate kinematics over the past 20 Myr. We reconstruct the history of opening of the Gulf of Aden, including the penetration of the Sheba Ridge into the African continent and the evolution of the triple junction since its formation. Magnetic data evidence three stages of ridge propagation from east to west. Seafloor spreading initiated ~20 Myr ago along a 200 km-long ridge portion located immediately west of the Owen fracture zone. A second 500 km-long ridge portion developed westward up to the Alula-Fartak transform fault before Chron 5D (17.5 Ma). Before Chron 5C (16.0 Ma), a third 700 km-long ridge portion was emplaced between the Alula-Fartak transform fault and the western end of the Gulf of Aden (45°E). Between 20 and 16 Ma, the Sheba Ridge propagated over a distance of 1400 km at an extremely fast average rate of 35 cm yr^{-1}. The ridge propagation resulted from the Arabia-Somalia rigid plate rotation about a stationary pole. Since Chron 5C (16.0 Ma), the spreading rate of the Sheba Ridge decreased first rapidly until 10 Ma and then more slowly. The evolution of the AOC triple junction is marked by a change of configuration around 10 Ma, with the formation of a new Arabia-India plate boundary. Part of the Arabian plate was then transferred to the Indian plate.

1. Introduction

[2] The Arabian plate began to separate from Africa in Oligocene times. Plate separation was initiated by continental rifting in the Gulf of Aden-Red Sea rift system and coincided with a strong magmatic surge in the Afar hot spot region 30 Myr ago [*Burke*, 1996; *Baker et al.*, 1996; *Hoffmann et al.*, 1997; *Rochette et al.*, 1997; *Ebinger and Sleep*, 1998; *Ukstins et al.*, 2002]. The separation occurred in the framework of closure of the Neo-Tethys Ocean subducting northeastward beneath Eurasia [*Dercourt et al.*, 1993; *Stampfli and Borel*, 2002; *Agard et al.*, 2005], a subduction still active today in the Makran region (Figure 1) [*Jacob and Quittmeyer*, 1979; *Vernant et al.*, 2004]. It is generally admitted that the Africa plate fragmentation resulted from the interplay between far-field extensional forces originated at the Neo-Tethyan subduction zone (slab-pull gravitational forces) and the impingement of the Afar mantle plume at the base of the African lithosphere [*Bott*, 1982; *Malkin and Shemenda*, 1991; *Zeyen et al.*, 1997; *Courtillot et al.*, 1999; *Jolivet and Faccenna*, 2000; *Bellahsen et al.*, 2003]. Arabia was torn off of Africa and driven northeastward by the Tethyan slab subducting beneath Eurasia. Following rifting of the African lithosphere, seafloor spreading initiated in early Miocene times in the eastern Gulf of Aden along the nascent Sheba Ridge [*Laughton et al.*, 1970; *Cochran*, 1981]. The spreading ridge propagated rapidly westward from the Owen fracture zone toward the Afar hot spot [*McKenzie et al.*, 1970; *Courtillot*,
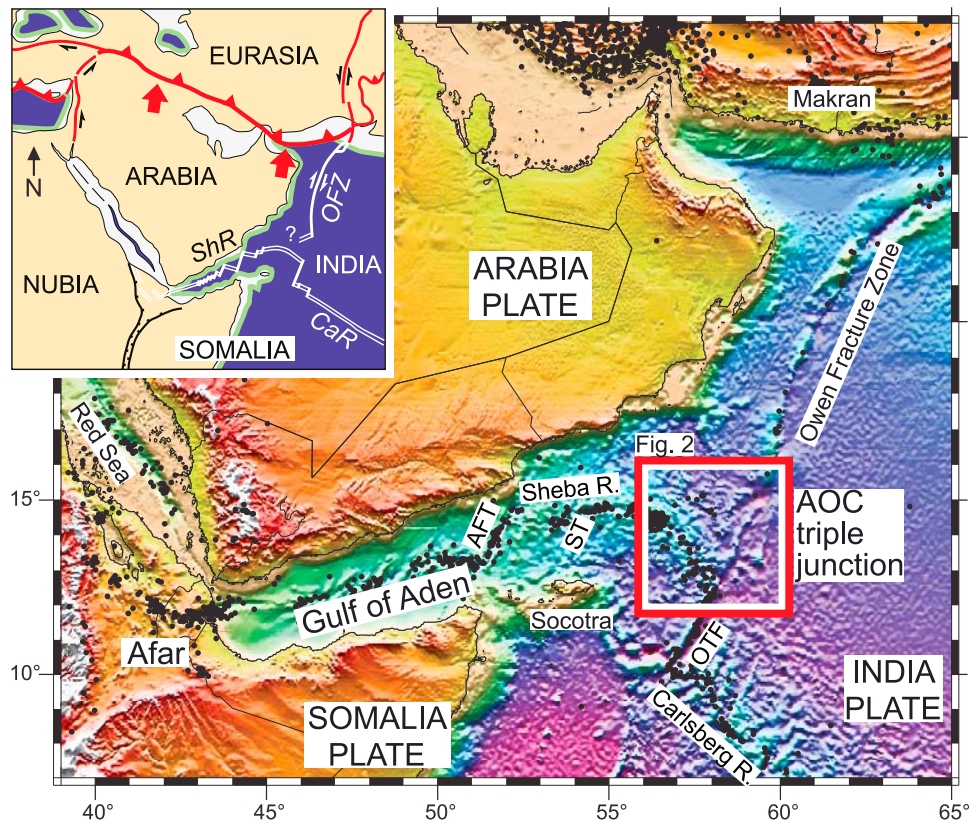

Figure 1. Geodynamic framework of the Gulf of Aden between the Afar hot spot and the Aden-Owen-Carlsberg (AOC) triple junction. Satellite altimetry data from *Sandwell and Smith* [1997] and shallow seismicity since 1973 from USGS/NEIC database (focal depth < 50 km; magnitude > 2). Inset shows the plate tectonics setting. AFT, Alula-Fartak transform fault; CaR, Carlsberg Ridge; OFZ, Owen fracture zone; OTF, Owen transform fault; R, ridge; ShR, Sheba Ridge; ST, Socotra transform fault.

1980; *Girdler*, 1991; *Manighetti et al.*, 1997; *Huchon and Khanbari*, 2003; *Hubert-Ferrari et al.*, 2003]. The connection of the Sheba Ridge with the Owen fracture zone and the Carlsberg Ridge formed the Aden-Owen-Carlsberg (AOC) triple junction between the Arabia, India, and Somalia plates [*Fournier et al.*, 2001].

[3] In this paper we first analyze marine magnetic data recently collected at the AOC triple junction on board the *Hydrographic and Oceanographic Vessel Beautemps-Beaupré* of the French Navy [*Fournier et al.*, 2008a, 2008b]. These data are crucial to decipher the first stages of opening of the eastern Gulf of Aden since they allow us to reconstruct the evolution of the AOC triple junction since its very early formation about 20 Ma ago. We then use all available magnetic profiles across the Gulf of Aden and the NW Arabian Sea to investigate the formation of the oceanic floor between the Arabian and Somalian plates. On the basis of this extensive magnetic data set, we establish a firm isochron pattern in the Gulf of Aden and calculate finite and stage rotation poles and their associated uncertainties. We further use this high-resolution kinematic model of the Arabia-Somalia relative motion to detail the evolution of the spreading rate and opening direction during the last 20 Myr. By closing the oceanic domain between conjugate magnetic anomalies, we restore the plate boundary configuration at each anomaly time and reconstruct the history of seafloor

spreading in the Gulf of Aden including the ridge propagation into the African continent and the evolution of its axial segmentation.

2. Regional Geodynamic Setting

2.1. Gulf of Aden

2.1.1. Main Tectonic Features

[4] Situated between southern Arabia and the Horn of Africa, the Gulf of Aden links the Ethiopian rift and the Red Sea with the Carlsberg Ridge in the NW Indian Ocean (Figure 1). Significant features of the seafloor topography of the Gulf of Aden and the NW Indian Ocean were delineated following the John Murray expedition in 1933–1934 [*Sewell*, 1934; *Farquharson*, 1936; *Wiseman and Sewell*, 1937] and the International Indian Ocean Expedition in 1959–1965 [*Heezen and Tharp*, 1964; *Laughton*, 1966a, 1966b]. They encompass a system of ridge segments with an axial valley marked by seismic activity that runs along the median line of the Gulf of Aden and the NW Indian Ocean [*Rothé*, 1954; *Ewing and Heezen*, 1960; *Sykes and Landisman*, 1964]. Southeast of Socotra Island, the Owen transform fault offsets by 330 km the Carlsberg Ridge and connects to the Sheba Ridge, which continues westward in the Gulf of Aden [*Matthews*, 1963, 1966; *Laughton*, 1966a; *Matthews et al.*, 1967; *Laughton et al.*, 1970]. In the eastern part of the

Gulf, the Sheba Ridge axis is offset by minor transform faults including Socotra transform (offset < 50 km; Figure 1). In the central part, it is offset over 200 km by one major transform fault, the Alula-Fartak transform fault [*Tamsett and Searle*, 1990; *Radhakrishna and Searle*, 2006]. In the western part, the ridge crest is offset by numerous NNE-SSW-trending structures early identified as left-stepping transform faults [*Laughton*, 1966b; *Tamsett and Searle*, 1988] with right-lateral motion [*Sykes*, 1968]. West of 46°E, the ridge axis becomes a shallow "gully" [*Farquharson*, 1936] running westward into the Gulf of Tadjura [*Choukroune et al.*, 1986, 1988; *Manighetti et al.*, 1998; *Audin et al.*, 2001, 2004].

2.1.2. Opening Rates and Directions and Oblique Rifting and Spreading

[5] *Le Pichon* [1968] used transform faults and magnetic isochrons to locate a first Euler pole describing the Arabia-Somalia relative motion at 26°N and 21°E, with a rotation angle of 7° to close the Gulf of Aden. *McKenzie et al.* [1970] obtained a similar rotation pole by fitting bathymetric contours (500 fathoms, i.e., 914 m) on each side of the Gulf (26.5°N, 21.5°E, rotation angle of 7.6°). Since then, several global [*Minster and Jordan*, 1978; *DeMets et al.*, 1990, 1994] and regional [*Chase*, 1978; *Le Pichon and Francheteau*, 1978; *Joffe and Garfunkel*, 1987; *Gordon and DeMets*, 1989; *Jestin et al.*, 1994; *Fournier et al.*, 2001] plate-motion models provided nearby instantaneous poles for the Arabia-Somalia motion. The spreading rate along the Sheba Ridge increases progressively from west to east from 1.6 cm yr^{-1} (full rate) at the entrance of the Gulf of Tadjura, to 2.4 cm yr^{-1} at the AOC triple junction.

[6] The Gulf of Aden is characterized by oblique opening. The present-day spreading direction is close to N25°E along the Alula-Fartak transform fault, as indicated by slip vectors of earthquake focal mechanisms (Global CMT catalog). The obliquity thus reaches 40° with respect to the N75°E mean trend of the Gulf of Aden. In the western part of the Gulf, obliquity is accommodated by en échelon faulting within the axial rift, with normal faults oblique to the ridge trend [*Dauteuil et al.*, 2001; *Fournier and Petit*, 2007]. Oblique spreading was preceded by oblique rifting of the Arabo-African lithosphere [*Beydoun*, 1970, 1982; *Platel and Roger*, 1989; *Roger et al.*, 1989; *Hughes et al.*, 1991; *Bott et al.*, 1992; *Birse et al.*, 1997; *Watchorn et al.*, 1998; *Fantozzi and Sgavetti*, 1998] marked by the development of a series of N100°–110°E-trending syn-rift grabens with a left-stepping en échelon arrangement [*Fantozzi*, 1996; *Brannan et al.*, 1997; *Lepvrier et al.*, 2002; *Bellahsen et al.*, 2006]. The along-strike 3-D evolution of the structure of the continental margins of the Gulf of Aden results from this syn-rift segmentation [*Fournier et al.*, 2004, 2007; *d'Acremont et al.*, 2005; *Petit et al.*, 2007; *Tibéri et al.*, 2007; *Lucazeau et al.*, 2008].

2.1.3. Age of the Oceanic Crust

[7] Oceanic crust has been identified from the interpretation of magnetic anomaly sequences up to anomaly 5 (11.0 Ma) first in the eastern [*Laughton et al.*, 1970] and then in the western [*Cochran*, 1981] Gulf of Aden. Beyond anomaly 5, *Cochran* [1982] and *Stein and Cochran* [1985] suggested the existence of a quiet magnetic zone with a crust having an oceanic seismic structure. More recently, anomaly sequence has been identified up to anomaly 5D (17.5 Ma) on both flanks of the Sheba Ridge east of the Alula-Fartak transform

fault [*d'Acremont et al.*, 2006], while anomaly 5C (16.0 Ma) has been recognized on the northern flank of the ridge immediately west of the Alula-Fartak transform fault [*Sahota*, 1990; *Huchon and Khanbari*, 2003]. These observations suggest a fast propagation of the Sheba Ridge and contradict the two-stage model of seafloor spreading proposed by *Girdler and Styles* [1974, 1978] for the western Gulf of Aden and Red Sea. On the basis of width measurements of the Gulf of Aden between escarpments of the conjugate margins (top and base), *Manighetti et al.* [1997] reconstructed a propagation history of the Aden rift tip starting from the Owen fracture zone prior to 30 Ma and reaching the western Gulf of Aden (45°E) about 18 Myr ago, with an average propagation rate of ~10 cm yr^{-1}. West of longitude 45°E, *Courtillot* [1982] and *Courtillot and Vink* [1983] showed, from the V-shape of magnetic anomalies interrupted at the continental margin, that since Chron 5 (11.0 Ma) the tip of the rift has propagated at a rate of 3 cm yr^{-1} in a westerly direction into the active Afar region [*Ebinger et al.*, 2008].

2.2. Aden-Owen-Carlsberg Triple Junction

[8] The Carlsberg Ridge, the Sheba Ridge, and the Owen fracture zone meet at the AOC triple junction. The Carlsberg Ridge [*Schmidt*, 1932; *Vine and Matthews*, 1963] was emplaced in the early Tertiary between the Seychelles and Indian continental blocks [*Patriat and Segoufin*, 1988; *Malod et al.*, 1997; *Dyment*, 1998; *Chaubey et al.*, 1998, 2002; *Miles et al.*, 1998; *Royer et al.*, 2002; *Minshull et al.*, 2008; *Collier et al.*, 2008; *Yatheesh et al.*, 2009]. It underwent a three-stage evolution with fast spreading stage (full-rate ~12 cm yr^{-1}) between 61 and 51 Ma (A27−A23; stage 1), followed by very slow divergence (<1.2 cm yr^{-1}) between 39 and 23 Ma (A18–A6b; stage 2) following the India-Eurasia collision, and by a slow spreading stage (~2.4 cm yr^{-1}) since 23 Ma (A6b) until present (stage 3) [*Mercuriev et al.*, 1996]. It is presently characterized by a nearly orthogonal accretion at a rate of ~2.2 cm yr^{-1} in its northwestern part [*Merkouriev and DeMets*, 2006]. The transition from stage 2 to stage 3 is coeval with (1) spreading initiation in the eastern Gulf of Aden and formation of the AOC triple junction and (2) a sharp decrease of the spreading rate along the Southwest Indian Ridge from slow to ultraslow at ~24 Ma [*Patriat et al.*, 2008]. The spreading rate along the eastern Sheba Ridge is currently slightly faster (2.4 cm yr^{-1}) than along the western Carlsberg Ridge. Arabia is thus moving northward more rapidly than India with respect to Somalia. The Arabia-India relative motion is taken up by the Owen fracture zone [*Matthews*, 1966; *Whitmarsh et al.*, 1974; *Whitmarsh*, 1979] and the Dalrymple trough [*McKenzie and Sclater*, 1971; *Minshull et al.*, 1992; *Edwards et al.*, 2000, 2008; *Gaedicke et al.*, 2002; *Ellouz-Zimmermann et al.*, 2007a, 2007b]. Between the Dalrymple Trough and latitude 15°N, the OFZ is characterized by a low seismic activity, and south of 15°N it is seismically quiet for about 250 km. The right-lateral sense of slip along this ~700 km long strike-slip plate boundary is attested by earthquake focal mechanisms [*Sykes*, 1968; *Quittmeyer and Kafka*, 1984; *Gordon and DeMets*, 1989] and geomorphologic offsets in the seafloor [*Fournier et al.*, 2008b]. Recently, we used three independent data sets (multibeam bathymetry, earthquakes focal mechanisms, GPS measurements at permanent sites) to show that the OFZ is a pure transform fault
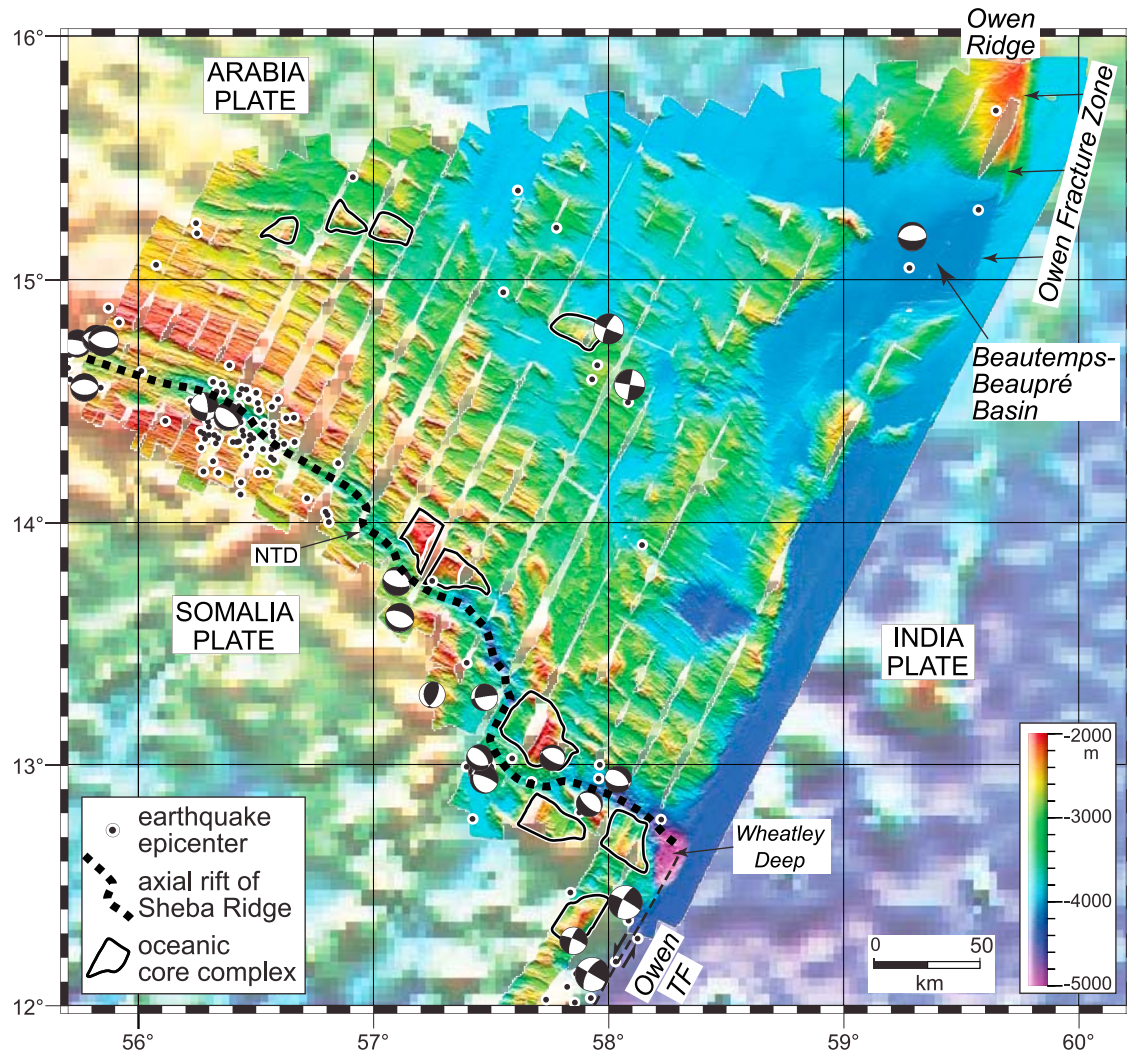
Figure 2. Multibeam bathymetric data of the AOC triple junction (location in Figure 1) superimposed on the world bathymetric map of *Sandwell and Smith* [1997] with shallow seismicity and earthquake focal mechanisms (Global CMT catalog). The map shows the northern flank of the Sheba Ridge and its axial rift, and the southern termination of the Owen fracture zone in the Beautemps-Beaupré Basin. NTD, nontransform discontinuity; TF, transform fault.

that follows a small circle centered on the Arabia-India rotation pole with a rate of motion of 2–4 mm yr^{-1} [*Fournier et al.*, 2008b].

3. Evolution of the AOC Triple Junction

3.1. Main Structural Features of the Triple Junction

[9] The axial rift of the Sheba Ridge surveyed during the AOC expedition exhibits morphologic, tectonic, and magmatic features changing from west to east (Figure 2) [*Fournier et al.*, 2008a]. In the western part, the rift is bounded by steeply dipping conjugate normal faults stepping down toward the spreading axis, marked by a continuous neovolcanic ridge. The overall structure is symmetric. East of a right-stepping nontransform discontinuity at 57°E [*Spencer et al.*, 1997], the rift becomes sinuous and deeper, and displays an asymmetric structure bounded alternatively to the north or to the south by flat-lying detachment faults associated with oceanic core complexes [e.g., *Cann et al.*,

1997; *Tucholke et al.*, 1998; *Cannat et al.*, 2006; *Ildefonse et al.*, 2007]. In this area the rift becomes less volcanic and displays only isolated volcanoes. At its eastern end the axial rift connects to the Owen transform fault (OTF) through a deep nodal basin (Wheatley Deep).

[10] In the northeastern part of the mapped area, the Arabia-India plate boundary is marked by a sharp, rectilinear, and vertical fault, the Owen fracture zone (Figure 2). This N10°E-trending fault crosscuts the Owen topographic ridge and offsets it dextrally over 12 km [*Fournier et al.*, 2008b]. The fault terminates to the south in the 50 km-wide and 120 km-long Beautemps-Beaupré Basin, bounded to the north and south by ~E–W normal faults. Immediately SW of the Beautemps-Beaupré Basin, anomalous fabric orientations in the seafloor indicate that E-W faults crosscut NW-SE faults and dykes formed at the Sheba Ridge axis [*Fournier et al.*, 2008a]. These faults indicate that intraplate extensional deformation propagated westward in the oceanic crust of northern flank of the Sheba Ridge. However, the
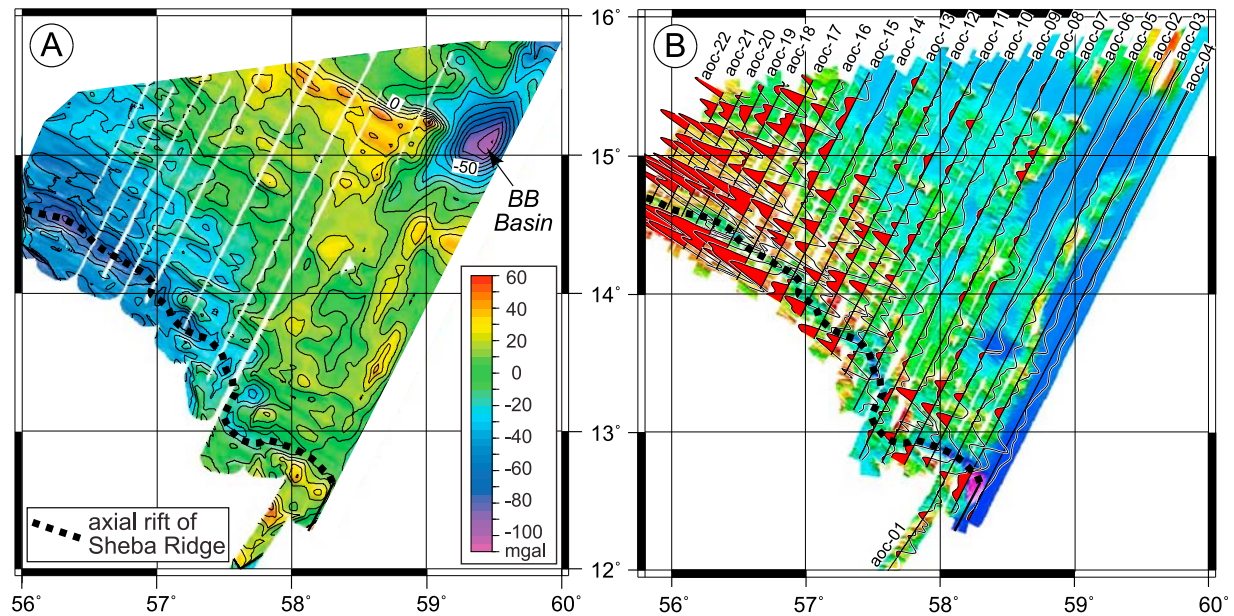
Figure 3. (a) Mantle Bouguer gravity map of the AOC triple junction computed using a mean density contrast of 1840 kg m^{-3} between the oceanic crust and water and of 300 kg m^{-3} between the crust and mantle. (b) Magnetic anomaly profiles plotted along ship tracks for AOC survey. High-amplitude magnetic anomalies coincide with a broad negative mantle Bouguer anomaly. Both gravity and magnetic data were acquired along the ship tracks with an original data spacing of 30 m along track and ~17 km (~9 nautical miles) between tracks.

extensional deformation zone does not reach the axis of the Sheba Ridge and the Arabia-India plate boundary seems to terminate into the Beautemps-Beaupré Basin some 250 km north of the Somalia plate boundary.

3.2. Eastern Sheba Ridge Segmentation Inferred From Gravity and Magnetics

[11] The eastern Sheba Ridge is made of two different portions showing negative mantle Bouguer anomaly and high-amplitude magnetics to the west and high Bouguer gravity and low-amplitude magnetics to the east, respectively (Figures 3a and 3b). To first order, mantle Bouguer anomaly variations may reflect crustal thickness variations: the relatively low anomaly in the western part of the Sheba Ridge probably indicates thicker oceanic crust there, associated with high magma supply and high-amplitude magnetics. The eastern part on the other hand, which is dominated by core complex exhumation, appears as less magmatic. Thus magmatic segmentation of the ridge revealed by gravity and magnetic data correlates with the tectonic style of the axial rift, symmetric to the west and asymmetric to the east, and corresponds to two modes of accretion operating along the ridge with or without detachment fault [*Escartin et al.*, 2008].

3.3. Magnetic Anomaly Identification

[12] We used the dense network of magnetic profiles of the AOC survey on the northern flank of the Sheba Ridge (Figure 4) combined with previous magnetic data on its southern flank (see section 4 for detail) to establish the isochron pattern in the eastern Gulf of Aden. Six profiles spanning the northern and southern flanks were reconstructed

in order to identify conjugate anomalies (Figure 5). Each magnetic profile was compared with a two-dimensional block model for identification of the anomalies. The model is based on the geomagnetic polarity timescale of *Cande and Kent* [1992, 1995] with astronomically calibrated reversal ages from *Lourens et al.* [2004]. Theoretical magnetic profiles were generated for variable half-spreading rates and a magnetized layer thickness of 400 m. For each profile, a sequence of anomalies starting at the rift axis and including anomalies 2Ay, 2Ao, 3A, 4A, 5, 5C, 5D, and 6 was picked (Figure 6). The correlations between adjacent profiles are very good in the western part of the AOC survey area, where the magnetic amplitude is high. Moreover, analysis of isochronous seafloor fabric generated by seafloor spreading from the multibeam bathymetric map strengthens correlations between magnetic profiles. However, in the eastern and northeastern part, the low magnetic amplitude of the anomalies makes recognition of some of them questionable or even impossible for several of the easternmost profiles. This is particularly true for anomaly 5E that we were unable to identify unambiguously (Figure 4).

[13] The isochron map reveals two main segments separated by a major right-stepping transform fault (Figure 6). This discontinuity offsets the ridge axis by about 25 km at 13.2°N and 57.5°E and it is bounded in its eastern inner corner by a large oceanic core complex with a southward dipping low-angle detachment fault. The trend of the corrugations (N26°E ± 2°) is consistent with that of the transform fault.

[14] Along the western segment, magnetic anomalies are identifiable from the central anomaly to anomaly 5D and even anomaly 6 in the eastern part (profiles aoc-09 to aoc-

Figure 4. AOC survey magnetic anomaly profiles projected along N27°E and aligned along the Sheba Ridge axis. Location of profiles is shown in Figure 3b. Theoretical anomaly profiles were generated using the magnetic inversion time scale of *Cande and Kent* [1995; see also *Sloan and Patriat*, 1992] with a magnetized layer of 400 m which follows the seafloor topography and a contamination factor of 0.7. The "y" or "o" suffixes of magnetic anomalies indicate the young or old edge of the chron, respectively.
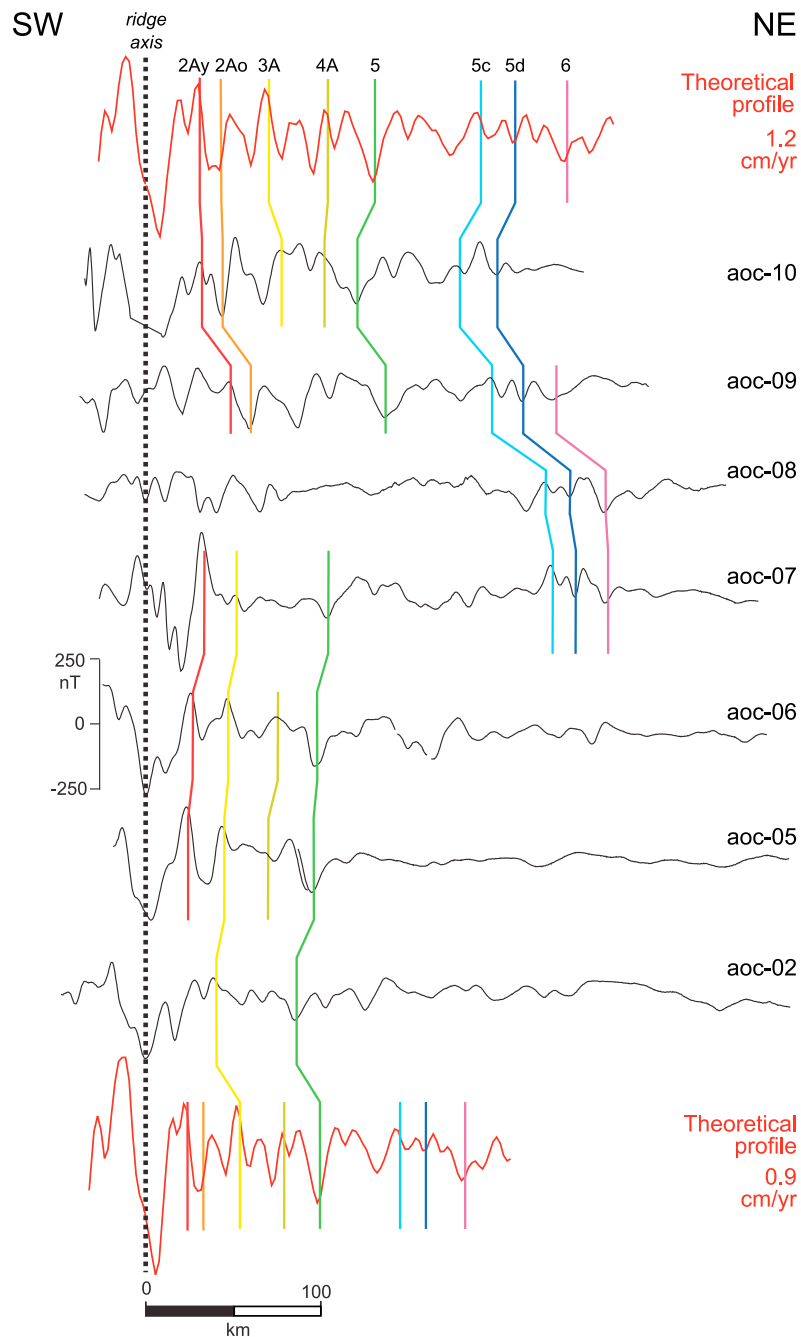
Figure 4. (continued)

22 in Figure 4). The isochrons 2Ay, 2Ao, and 3A are linear and parallel to the present-day spreading axis. Older isochrons (chrons 4A to 5D or 6) are offset by fracture zones (inset in Figure 6). A major change in the geometry of the axis therefore occurred between chrons 4A and 3A. Since Chron 5 (11.0 Ma), the spreading rate along the western segment has remained stable at 2.4 cm yr^{-1} (full rate), decreasing to 2.3 cm yr^{-1} westward toward the rotation pole

(Figure 5). Spreading is asymmetric with a half-spreading rate higher to the north (1.3–1.4 cm yr^{-1}) than to the south (0.9–1.0 cm yr^{-1}; Figure 5).

[15] The eastern segment is 100 km-long between the Owen transform fault and the 57°30′E transform fault. On the southern flank, magnetic anomalies are identified from anomaly 2Ay to 6, whereas on the northern flank the anomaly sequence is recognized with confidence up to

Figure 5. Six full magnetic anomaly profiles across the eastern Gulf of Aden reconstituted from V3502 and V3617 (R/V Vema), WI330381 (R/V Wilkes), DD671 (Russian ship), and AOC (R/V Beautemps-Bea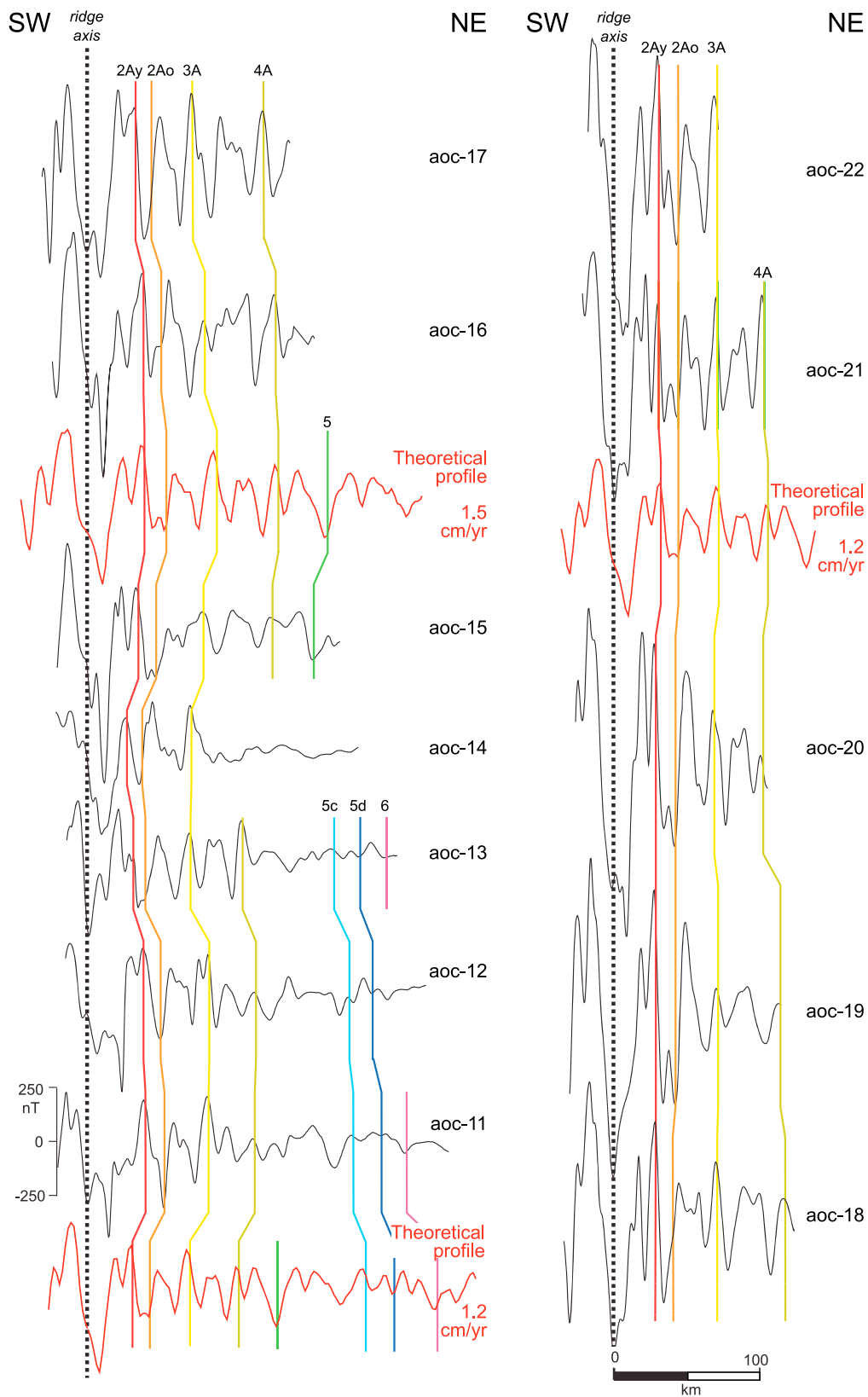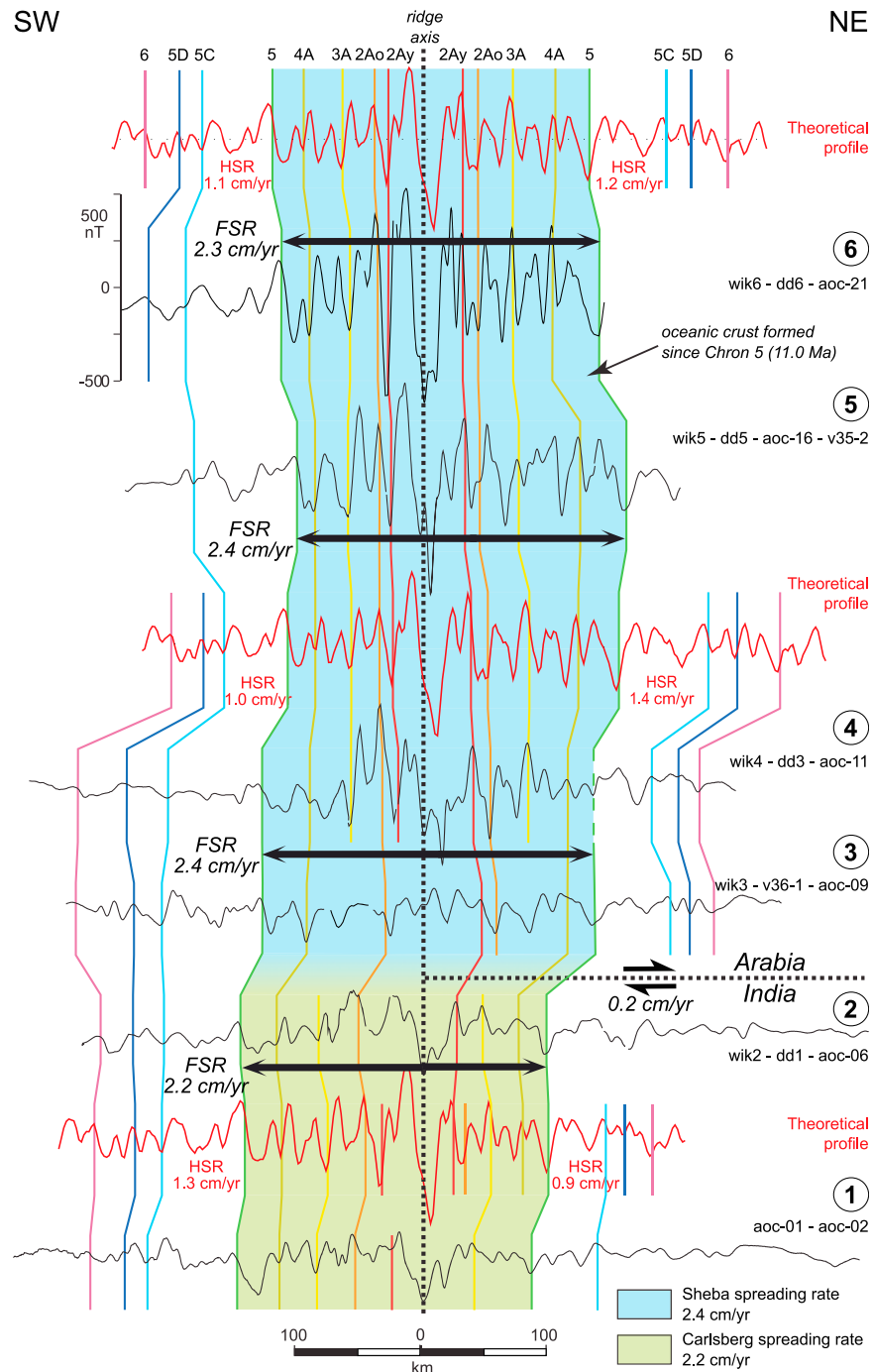upré) surveys. The profiles are projected along N27°E and aligned along the Sheba Ridge axis. Location of profiles is shown in Figure 6. Since Chron 5 (11.0 Ma), oceanic floor was generated at a full spreading rate of 2.4 cm yr^{-1} along the western segment (in blue referred to as "Sheba rate") and of 2.2 cm yr^{-1} along the eastern segment (in green referred to as "Carlsberg rate"). The relative motion of 2 mm yr^{-1} is accommodated by right-lateral slip along the transform zone between the two segments. Same legend as Figure 4. HFS, half-spreading rate for theoretical profiles; FSR, full spreading rate.

anomaly 5 only (profiles aoc-01 to aoc-07 in Figure 4). Moreover, anomaly 2Ao is missing on the northern flank due to a ridge jump toward the north between Chron 2Ao and 2Ay. Since Chron 5, the spreading rate along the eastern segment is 2.2 cm yr^{-1} (full rate). Spreading is asymmetric with a half-spreading rate higher to the south (1.3 cm yr^{-1}) than to the north (0.9 cm yr^{-1}; Figure 5), i.e., opposite to the western segment.
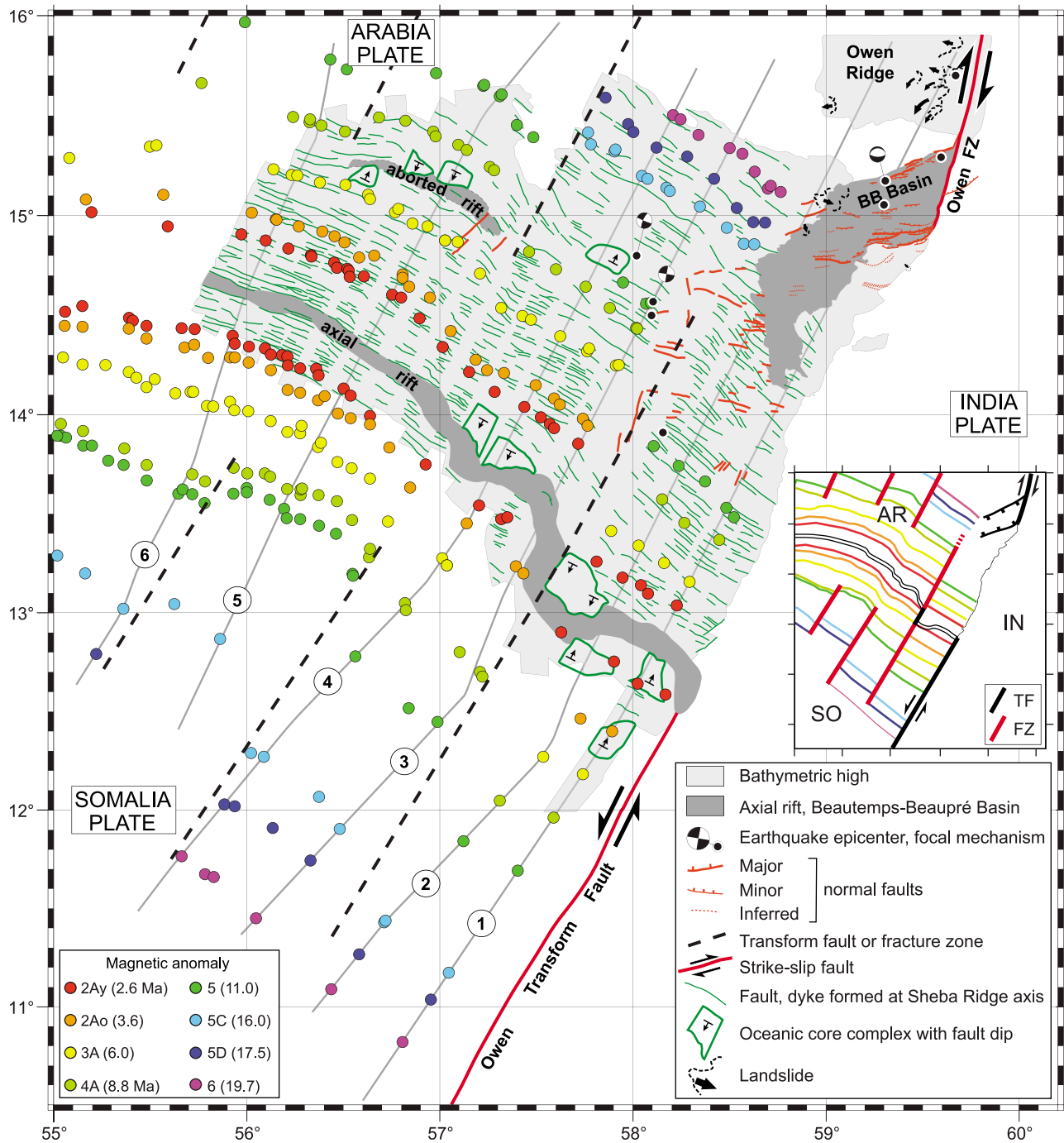
Figure 6. Magnetic anomaly picks plotted on the structural map of the AOC triple junction. Two segments separated by a major transform fault are recognized. Along the western segment, magnetic anomalies are identified from anomaly 2Ay to 6 on both flanks of the ridge. Along the eastern segment, magnetic anomalies are identified from anomaly 2Ay to 6 on the southern flank and from anomaly 2Ay to 5 on the northern one. In the central part of the western segment, the anomaly 5, which is an important marker usually recognized with certainty, is not clearly identified (profiles aoc-11 to aoc-14 in Figure 4). To the west of the Beautemps-Beaupré Basin, NW-SE-trending faults and dykes formed at the Sheba Ridge are crosscut by E-W faults, suggesting that the extensional deformation has propagated westward. Inset shows the isochron map with the present-day geometry of plate boundaries. AR, Arabian plate; FZ, fracture zone; IN, Indian plate; SO, Somalia plate; TF, transform fault.

Figure 7. Four-stage evolution of the AOC triple junction at chrons 5C, 5, 3A, and present. The configuration of the junction before and after the change of geometry of the Arabia-India plate boundary is shown with the corresponding velocity space diagrams. The change in configuration was induced 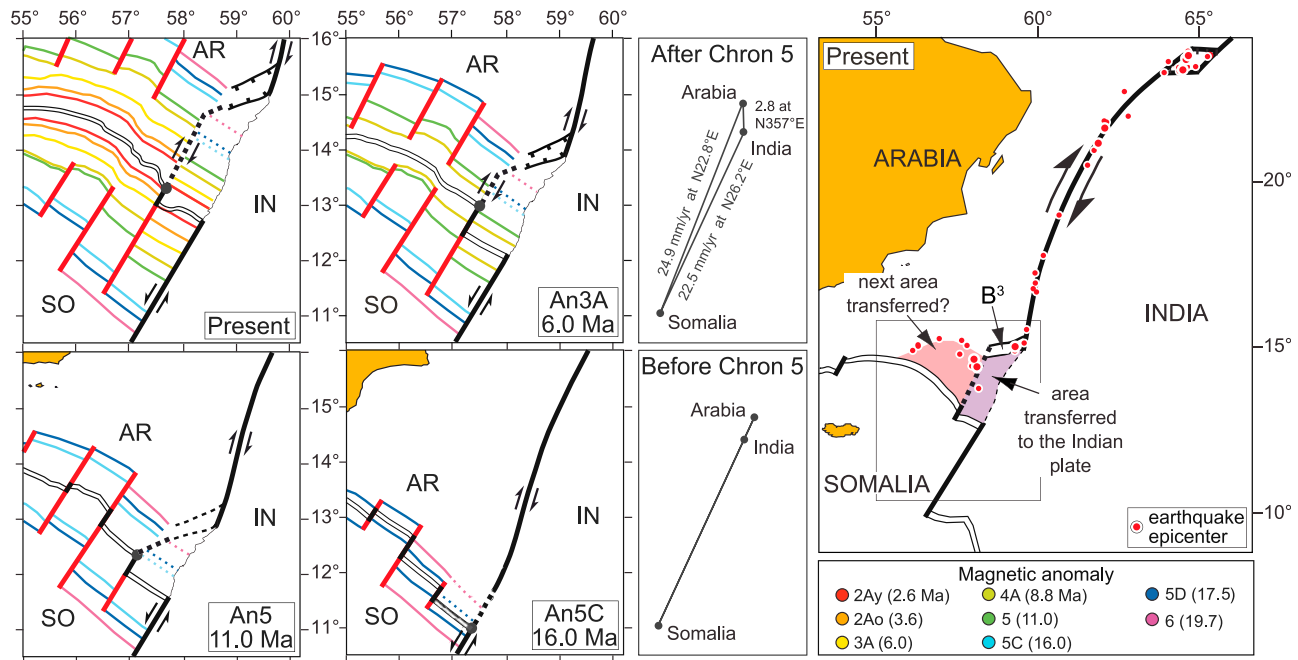by a regional kinematic reorganization about 10 Ma ago (Chron 5), which initiated the formation of the Beautemps-Beaupré Basin (B^3). Seismicity data suggest that, presently, a new plate boundary is developing to the west of the Beautemps-Beaupré Basin. In the near future, a larger area of the Arabian plate could be transferred to the Indian plate. AR, Arabian plate; IN, Indian plate; SO, Somalia plate.

3.4. Present-Day Configuration and Past Reconstruction of the Triple Junction

[16] Since Chron 5, the spreading rate is 2 mm yr^{-1} slower along the easternmost segment of the Sheba Ridge than along the segment immediately west (Figure 5). This rate difference between the two segments is accommodated by right-lateral slip along the northward extension of the 57°30′E transform fault (Figures 6 and 7). On the bathymetric map, this extension corresponds to a ~30 km-wide deformation zone, where seafloor fabric is rotated clockwise in agreement with dextral shear (Figure 6). Thus the Arabia-India plate boundary follows the 57°30′E transform zone, then passes through the Beautemps-Beaupré Basin, and joins the southern end of the Owen fracture zone. Since Chron 5, the spreading rate of the easternmost segment of the Sheba Ridge is similar to the spreading rate of the northwestern Carlsberg Ridge (2.2 cm yr^{-1}) [*Merkouriev and DeMets*, 2006]. Since then, this segment therefore pertains to the Carlsberg Ridge and is part of the India-Somalia plate boundary. Consequently, a portion of the Arabian plate has been transferred to the Indian plate (Figure 7) [*DeMets*, 2008].

[17] The transform boundary is however almost seismically quiet (Figures 2 and 7). At its northern end, one strike-slip focal mechanism at 14.57°N and 58.09°E (Global CMT catalog, 5 December 1981) is consistent with dextral motion along a N10°E-trending vertical fault plane (Figure 6). Most earthquakes are however localized in the western prolongation of the Beautemps-Beaupré Basin, as if a new plate boundary was developing there (Figure 7). A larger area of the Arabian plate could then be transferred in the future to the Indian plate.

[18] The evolution of the AOC triple junction can be reconstructed from magnetic data since its formation about 20 Myr ago, shortly before Chron 6. A major change of configuration occurred when the Beautemps-Beaupré Basin developed. This change occurred at the time of the latest kinematic reorganization in the Indian Ocean corresponding to the onset of intraplate deformation in the India-Australia plate dated at 7.5–8 Ma by ODP drillings [*Cochran*, 1990; *Chamot-Rooke et al.*, 1993; *Delescluse and Chamot-Rooke*, 2007], an age recently reappraised at 9 Ma [*Delescluse et al.*, 2008], and to a kinematic change along the Carlsberg Ridge between 11 and 9 Ma [*Merkouriev and DeMets*, 2006; *Fournier et al.*, 2008b]. A four-stage evolution of the triple junction at chrons 5C, 5, 3A, and present has been reconstructed in Figure 7 using India-Somalia rotation poles for the eastern segment of the Sheba Ridge since Chron 5 [*Merkouriev and DeMets*, 2006] and Arabia-Somalia poles for the western segment (this study, next section). The change in the geometry of the Arabia-India plate boundary occurred around Chron 5. Before Chron 5, the Owen fracture zone was probably connected directly to the Owen transform fault. The triple junction was located at the junction between the Owen fracture zone, the Owen transform fault, and the Sheba Ridge with a ridge-fault-fault (RFF) geometry. The RFF configuration, with two transform faults having the same strike and a flat velocity triangle, was stable (Figure 7) [*McKenzie and Morgan*, 1969; *Patriat and*

Courtillot, 1984]. Since Chron 5, the new triple junction appears to be stable, although a ridge jump occurred along the eastern segment between Chron 2Ao and 2Ay. The velocity space diagram of the junction is almost flat because the spreading rates and directions along the eastern Sheba and western Carlsberg ridges are very close. Transtension is predicted along the transform zone between the two ridge segments (N-S motion along the N27°E-trending discontinuity). Seismicity data suggest, however, that a change of configuration is presently occurring and that the current triple junction is in a transient state.

4. Arabia-Somalia Plate Kinematics

4.1. Pattern of Magnetic Anomalies

[19] All available ship tracks for magnetic profiles used in this study are located in Figure 8a. The main magnetic surveys in the Gulf of Aden are the cruises of RRS *Shackleton* [*Girdler and Styles*, 1978; *Girdler et al.*, 1980; *Tamsett and Girdler*, 1982; *O'Reilly et al.*, 1993], R/V *Vema* [*Cochran*, 1981, 1982; *Stein and Cochran*, 1985], and a Russian research vessel [*Solov'ev et al.*, 1984] in the late seventies, and more recently the cruises of R/V *L'Atalante* [*Audin et al.*, 2001; *Hébert et al.*, 2001; *Dauteuil et al.*, 2001], R/V *Marion Dufresne* [*Leroy et al.*, 2004; *d'Acremont et al.*, 2005, 2006; *Fournier et al.*, 2007], and R/V *Beautemps-Beaupré* [*Fournier et al.*, 2008a, 2008b]. These surveys, completed by supplementary profiles in the Gulf of Aden (Figure 8a), provide a dense set of profiles in the direction of seafloor spreading, i.e., favorably oriented for magnetic anomaly identification.

[20] The anomaly intensities have been plotted and contoured in Figure 8b, where the profile spacing permits it. The pattern of seafloor-spreading anomalies parallel to the ridge axis is revealed. The axial rift is characterized by an intense negative anomaly often reaching −1000 nT, with larger amplitude in the western Gulf of Aden than in the east [*Tamsett and Girdler*, 1982]. In the eastern part of the Gulf, the anomalies are well developed and a regular pattern of alternating linear anomalies trending ~N110°E is observed.

4.2. Magnetic Anomaly Identification

[21] Magnetic anomalies were identified on each profile and the anomaly picks were plotted to produce an isochron map (Figure 8c). In the eastern part of the Gulf of Aden, magnetic anomalies have been identified from anomaly 2A to 6 on both flanks of the Sheba Ridge (Figure 6). Further west, up to the Alula-Fartak transform fault, conjugate sequences of anomalies have been identified up to anomaly 5D (17.5 Ma). West of the Alula-Fartak transform fault, magnetic anomalies are generally of smaller amplitude and more difficult to interpret than in the east. Nevertheless, from the Alula-Fartak transform fault to 45°E, we could identify with confidence a continuous anomaly sequence from the axial anomaly to anomaly 5C on both flanks of the ridge. Anomaly 5C is consistently located at the foot of the escarpment of the continental margin, which coincides with the 1500 m isobath in the western Gulf of Aden. Magnetic data thus indicate that, since Chron 5C (16.0 Ma), oceanic floor was emplaced in most of the Gulf of Aden and that the opening of the ocean basin was a continuous process.

4.3. Finite Rotation Pole Locations

[22] The new picking was used to compute reconstruction poles for the Arabia-India plate motion. We carried out a systematic search in a three-dimensional space for the best latitude, longitude, and rotation angle. The cost function was taken as the sum of the surfaces delineated by nonrotated and rotated neighbors [e.g., *McKenzie and Sclater*, 1971; *Patriat*, 1987]. Errors were obtained using a Monte-Carlo scheme. For one given chron, we allow all pickings to randomly move away from their original positions using a Gaussian function with standard deviation sigma. A new pole is then recomputed. At the end of the process, we obtain a population of poles from which the centroid is taken as the best pole. Errors are extracted from the variances-covariances matrix, in terms of length and orientation of the error ellipse axes, and error on the rotation angle. In practical way, sigma was set to 1.67 km, a value provided by *Merkouriev and DeMets* [2006] from their analysis of the Carlsberg Ridge magnetics, which represents their best estimate of random noise in anomaly picking. *Merkouriev and DeMets* [2006] also mentioned other sources of error including systematic outward displacement of magnetic anomalies [*DeMets and Wilson*, 2008; *Merkouriev and DeMets*, 2008] and segment-specific systematic errors. We could not however take into account these errors in our analysis, which is limited by the number of pickings available (less than 200 pickings for each isochron; Table 1 and Data Set S1 in the auxiliary material) and the small number of segments compared to their study.[1] We empirically found that the centroid did not change significantly once several hundred iterations were performed. For each isochron, we realized more than 1000 iterations to determine the uncertainties of the rotation pole.

[23] We used a different strategy to calculate the reconstruction pole for Chron 6. Owing to the short length of isochrons 6, we were unable to unambiguously determine both the position and the rotation angle. We noticed however that the reconstruction pole of *McKenzie et al.* [1970] was compatible with the closure of isochrons 6 provided a slight increase of the rotation angle (7.84 instead of 7.6°, which corresponds to fitting the 500 m bathymetric contours instead of 500 fathom, i.e., 914 m). One implication is that the initiation of seafloor spreading occurred shortly before Chron 6, unless spreading started at a very slow rate.

[24] We plotted in Figure 9a the seven poles of reconstruction from Chron 2Ay (2.6 Ma) to Chron 5D (17.5 Ma) with their 95% confidence interval (Table 1). Also shown is the reconstruction pole of *McKenzie et al.* [1970] used for Chron 6. Error ellipses are larger for the oldest pole (Chron 5D), because only the eastern part of the Gulf of Aden was oceanized at that time, and for the youngest pole (Chron 2Ay), because of the small rotation angle. At 4-sigma level, all poles overlap which could preclude any discussion of migration through time. However, the reconstruction poles do not seem to be randomly distributed. Most of them are aligned along a great circle and migrate southeastward toward the Gulf of Aden from the older to the younger. A noticeable exception is the pole for Chron 2Ay (2.6 Ma), which is apart from the other poles.

---

[1]Auxiliary material data sets are available at ftp://ftp.agu.org/apend/jb/2008jb006257. Other auxiliary material files are in the HTML.
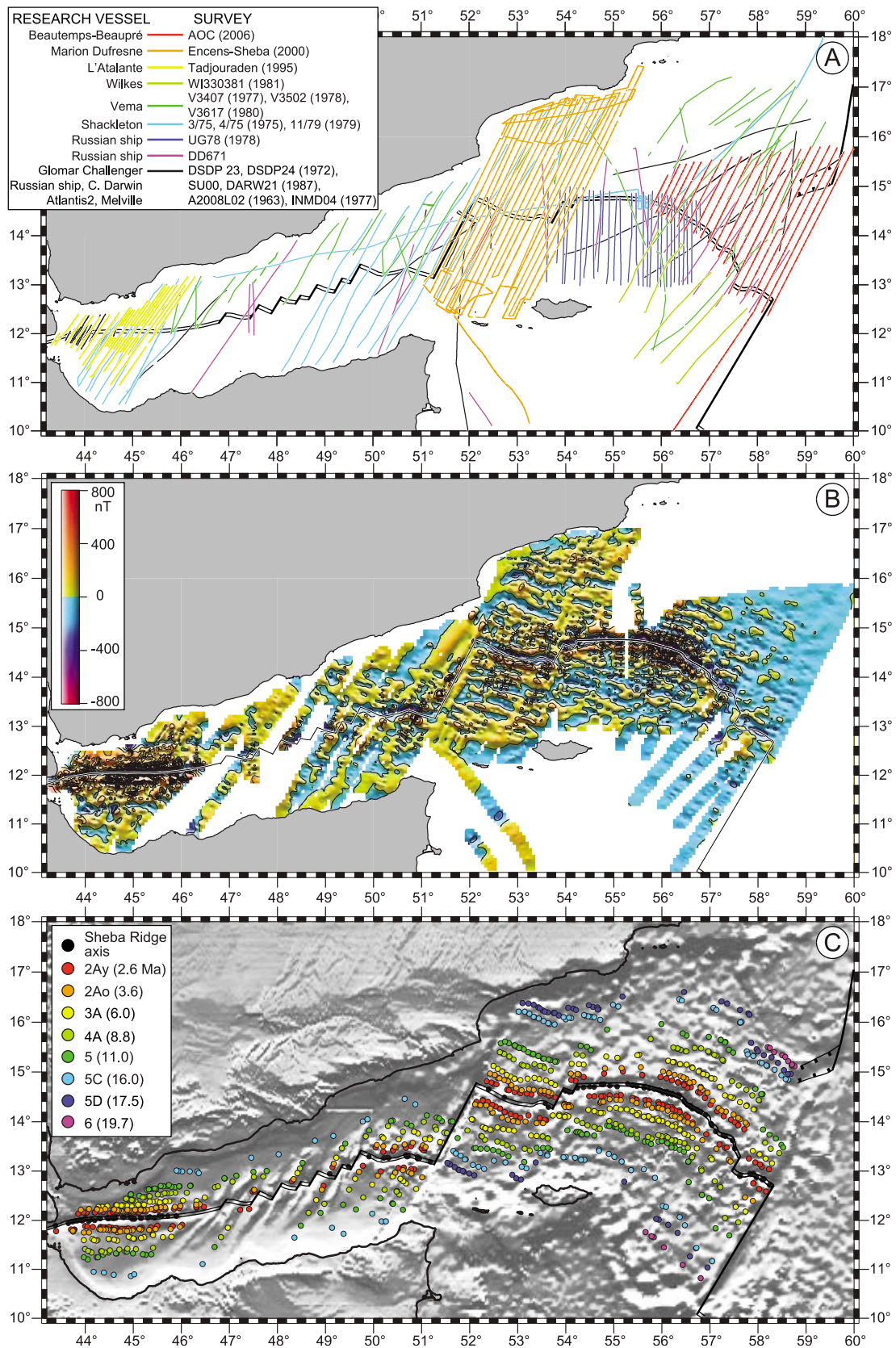
Figure 8. (a) Location of ship tracks for magnetic profiles used in this study. (b) Contoured magnetic anomaly amplitude map of the Gulf of Aden. Contour interval, 200 nT. (c) Magnetic anomaly picks including the central anomaly and anomalies 2Ay, 2Ao, 3A, 4A, 5, 5C, 5D, and 6. Anomaly 5C (16.0 Ma) can be traced in most of the Gulf of Aden.

Table 1. Arabia-Somalia Finite Rotations, Covariances, and Error Ellipses[a,b]

Chron	Age (Ma)	Number of Pickings[b]	Latitude (°N)	Longitude (°E)	ω (deg)	Covariances						Error Ellipse		
						a	b	c	d	e	f	σ_{max}	σ_{min}	ζ_{max}
C2An.1y	2.581	183	23.67	22.21	0.939	22.2	25.3	2.2	29.3	2.7	4.3	1.98	0.77	−51
C2An.3o	3.596	173	21.28	28.50	1.619	27.7	32.1	0.9	37.8	1.6	9.5	1.26	0.57	−33
C3An.1y	6.033	167	25.46	25.41	2.398	22.0	26.0	6.2	31.5	7.6	6.6	0.70	0.34	−54
C4Ay	8.769	137	22.56	27.71	3.985	25.5	29.7	6.5	35.7	7.3	4.9	0.41	0.16	−55
C5n.2o	11.040	153	23.88	26.66	4.740	34.8	41.4	9.8	50.7	11.9	5.7	0.42	0.14	−60
C5Cn.1y	15.974	102	25.85	25.40	6.853	84.0	100.9	20.8	123.0	25.5	11.0	0.49	0.13	−57
C5Do	17.533	55	26.10	22.98	7.283	2615	3612	1357	4995	1878	714	2.93	0.18	−79
C6no	19.722	15	26.46	21.66	7.830	-	-	-	-	-	-	-	-	-

[a]Rotations reconstruct the Somalia plate relative to the Arabia plate; a, b, c, d, e, and f are the Cartesian elements of the covariance matrix in units of 10^{-8} rad^2, where a, d, and f are the diagonal elements with the three axes of the Cartesian frame defined as (0°N, 0°E), (0°N, 90°E), and 90°N. One-sigma, two-dimensional, error ellipses calculated in the plane tangent to Earth's surface are given by their great (σ_{max}) and small (σ_{min}) semiaxis length (in degrees) and by the azimuth (ζ_{max}) of the great axis (in degrees clockwise from north).
[b]Pickings are provided in Data Set S1 in the auxiliary material.

4.4. Evolution of the Relative Plate Motion

[25] The finite poles were used to calculate a series of stage poles (Table 2) and follow the evolution of the opening rate through time at three points of the Sheba Ridge in the western (12°N, 45°E), central (14°N, 52°E), and eastern (13°N, 58°E) Gulf of Aden (Figure 10). Spreading started about 20 Ma ago and spreading rate increased to a value of about 3 cm yr^{-1} between chrons 5D and 5C (17.5–16 Ma). Since then, the spreading rate has decreased continuously, first rapidly by as much as 30% in the early stages (17–10 Ma) and then slowly (less than 10%) during the last 10 Myr. A slight change in spreading direction is observed around 10 Ma with a counterclockwise rotation of the spreading direction (Figure 11b).

5. Discussion: Implications for the Opening of the Gulf of Aden

5.1. Three-Stage Propagation of the Sheba Ridge

[26] Magnetic data allow us to decipher the progressive penetration of the Sheba Ridge into the African continent. The isochron map shows three stages of propagation of the ridge (Figure 11). The first stage corresponds to the emplacement ~20 Myr ago, shortly before Chron 6 (19.7 Ma), of a 200 km-long ridge portion trending N130°E southeast of Socotra Island (Figure 12). It was followed by the development before anomaly 5D (17.5 Ma) of a 500 km-long ridge portion up to the Alula-Fartak transform fault, composed of six segments separated by five transform faults (offset < 50 km; Figure 12). Ridge propagation apparently stopped for about 1 Myr at the Alula-Fartak transform fault and resumed shortly before anomaly 5C (16.0 Ma) with the formation of a third ridge portion in the western Gulf of Aden between the Alula-Fartak transform fault and 45°E. This 700 km-long ridge portion was segmented by a series of at least eight left-stepping transform faults (magnetic data are however not dense enough to reconstruct the detailed geometry of the axis at Chron 5C). Propagation of the Sheba Ridge into the Gulf of Aden was completed around 16 Ma (Figures 11 and 12). From then on, oceanic floor was emplaced in most of Gulf of Aden. The propagation of the ridge over a distance of 1400 km occurred within a short period of time not exceeding 4 Myr (between 20 and 16 Ma) at an extremely fast average rate of 35 cm yr^{-1}. The western

ridge portion formed at an even faster rate, greater than 45 cm yr^{-1} (700 km in less than 1.5 Myr between chrons 5D and 5C). Because of the very fast ridge propagation rate and the limited temporal resolution of magnetic anomalies (~1 Ma), we cannot determine whether the propagation has been continuous or discontinuous. However, west of the Alula-Fartak transform fault, the anomaly 5C is located at the foot of the escarpment of the continental margin and there is apparently no space free for additional oceanic crust beyond anomaly 5C. The Alula-Fartak transform fault therefore appears as a major structural and probably temporal discontinuity. Ridge propagation rates of the same order are observed in back-arc setting in the Woodlark Basin (14 cm yr^{-1}) [*Taylor et al.*, 1995, 1999], the Lau-Havre-Taupo Basin (11 cm yr^{-1}) [*Parson and Hawkins*, 1994; *Parson and Wright*, 1996], and the Shikoku Basin (27–30 cm yr^{-1}) [*Chamot-Rooke et al.*, 1987; *Sdrolias et al.*, 2004]. According to our results, the pole of opening did not change significantly during the short time span of ridge propagation. The propagation thus results of the rotation of two rigid plates, Arabia and Somalia, about a relatively stationary pole located to the northwest of the propagating ridge, as in the propagating rift model proposed by [*Martin* 1984]. This passive process is different from the "forced" propagating rift model [*Hey*, 1977], in which the relative rotation pole progressively migrates along with the tip of the propagator [*Hey et al.*, 1980].

5.2. Transition From Continental Extension to Seafloor Spreading

5.2.1. Timing and Pattern of Rifting

[27] Seafloor spreading in the Gulf of Aden was preceded by rifting of the African continental lithosphere. The timing of rifting is ascertained by the analysis of Tertiary sedimentary series trapped in the coastal grabens of the Gulf. These sequences are reliably correlated on the conjugate margins on the basis of biostratigraphic and facies analyses [*Beydoun*, 1970; *Fantozzi and Sgavetti*, 1998]. Typical synrift deposits of late Oligocene to early Miocene age are recognized in the coastal grabens, corresponding to the Shihr Group in Yemen [*Beydoun*, 1964; *Watchorn et al.*, 1998] and Socotra [*Beydoun and Bichan*, 1969; *Samuel et al.*, 1997], the Guban Series in Somalia [*Abbate et al.*, 1993; *Fantozzi and Ali Kassim*, 2002], and the Mughsayl Formation in Oman [*Roger et al.*, 1989; *Platel et al.*, 1992]. They consist in calci-
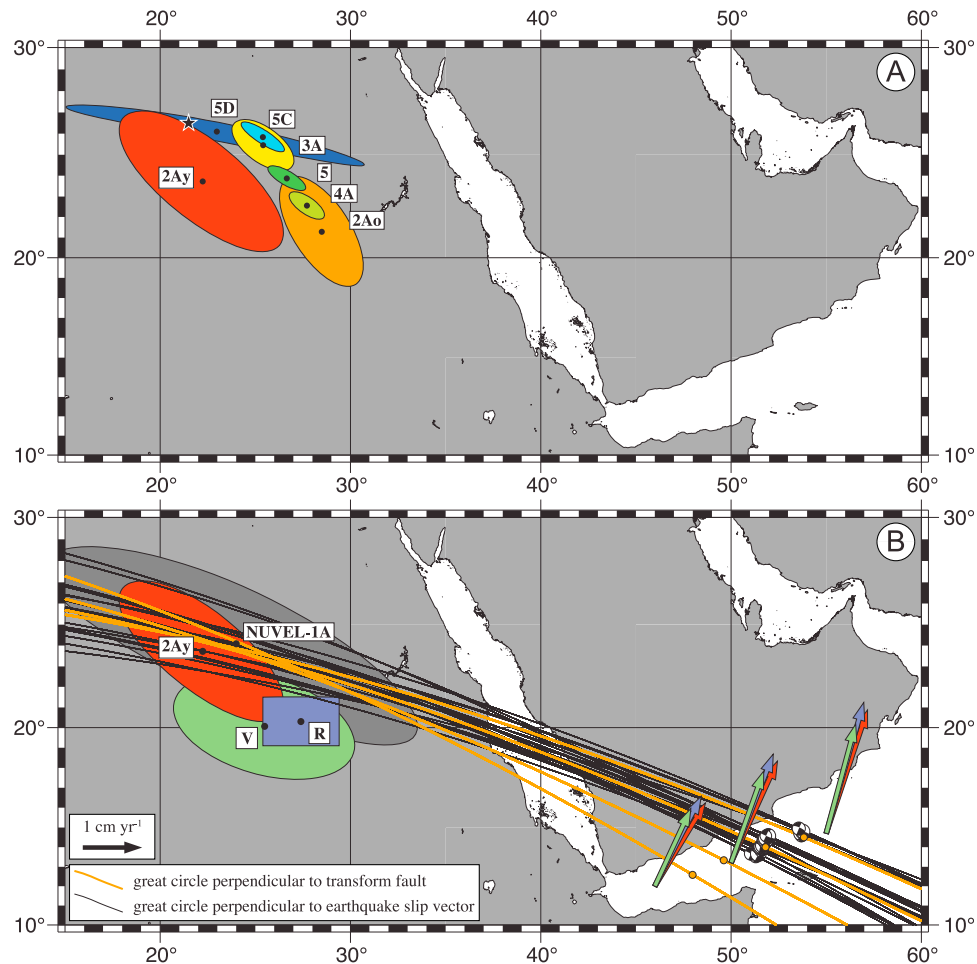
Figure 9. (a) Kinematics of the Gulf of Aden calculated from seafloor spreading magnetic anomalies: Arabia-Somalia finite rotation poles with their 2-sigma error ellipse (Table 1) and finite rotation pole to close the Gulf of Aden (star) [*McKenzie et al.*, 1970]. Since Chron 5D, the rotation poles migrated southeastward toward the Gulf of Aden. (b) Arabia-Somalia instantaneous kinematics: comparison between "geodetic" and "geologic" kinematics with an independent data set (azimuths of transform faults and earthquake slip vectors). Rotation poles calculated from GPS data (R [*Reilinger et al.*, 2006] and V [*Vigny et al.*, 2006]) and from magnetic data (NUVEL-1A and Chron 2Ay) are plotted with their 2-sigma error ellipses, together with rates predicted along the Sheba Ridge (arrows). Great circles perpendicular to transform faults and earthquake slip vectors (Table 3) should intersect near the rotation pole [*Morgan*, 1968].

turbidic slope deposits including megabreccia, debris flows, and olistolitic material transported from the adjoining shelf, which result from the collapse and subsidence of the margins and attest of rapid deepening of depositional environment. The upper age limit of the syn-rift succession is well constrained around 20 Ma (between 21.1 and 17.4 Ma) [*Watchorn et al.*, 1998]. The onset of rifting is poorly dated around Oligocene based on stratigraphic [*Platel and Roger*, 1989; *Bott et al.*, 1992; *Hughes and Beydoun*, 1992; *Fantozzi*, 1996; *Watchorn et al.*, 1998] and fission track dating [*Menzies et al.*, 1997; *Abbate et al.*, 2001; *Gunnell et al.*, 2007]. The timing of rifting in the Red Sea is similar to the Gulf of Aden, although it has been suggested that rifting may have started slightly later (see synthesis in the work of *Bosworth et al.* [2005]). Recent studies of the northern main Ethiopian rift suggest that extension started there after 11 Ma [*Wolfenden et al.*, 2004; *Corti*, 2008; *Keranen and*

Klemperer, 2008]. In this case, the kinematics of opening of the Gulf of Aden would also apply to the Red Sea opening for the 20 to 11 Ma period. This cannot be tested further in the Red Sea since seafloor spreading started only 4–5 m.y. ago and in the southern part only [*Cochran and Karner*, 2007].

[28] Rifting in the Gulf of Aden was achieved by the formation of multiple left-stepping grabens trending N100°E–N110°E and aligned along a direction converging toward the Afar hot spot (Figure 12) [*Fantozzi*, 1996; *Huchon and Khanbari*, 2003; *Bellahsen et al.*, 2006]. The en échelon arrangement of the grabens attests of an oblique rifting with a dextral shear component parallel to the proto-Gulf of Aden. The total width of the shear deformation zone encompassing the grabens is ~200 km. The oblique rifting in the Gulf of Aden contrasts with the orthogonal rifting in the Red Sea strongly controlled by preexisting basement faults [*Hughes et al.*, 1991]. Rifting in the Gulf of Aden ultimately resulted
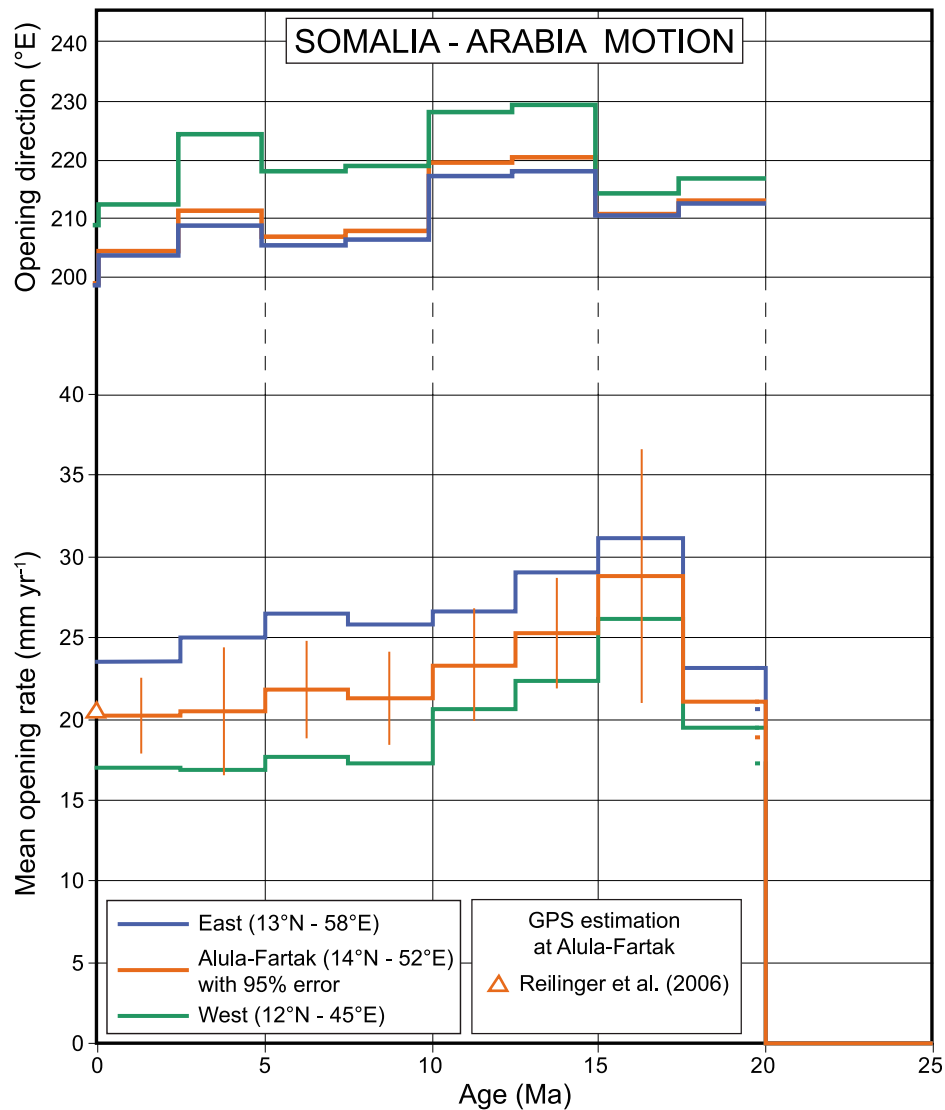
Figure 10. Variation of the opening rate and direction (with respect to Arabia) through time for three different portions of the accreting boundary: western (12°N, 45°E), central (14°N, 52°E; Alula-Fartak transform fault), and eastern (13°N, 58°E; AOC triple junction area) Gulf of Aden. Stage poles every 2.5 Myr are derived from the original stage poles (Table 2). The slow and gradual decrease of the spreading rate during the last 10 Myr is not in line with a 15–20% decrease during the last 3 Myr, as suggested by GPS data [*Vigny et al.*, 2006].

in the breakup of the continental lithosphere and the progressive emplacement of the Sheba Ridge. Oceanic accretion was initiated in the easternmost Gulf of Aden near the Owen fracture zone and propagated rapidly westward within the rift zone. For each ridge portion, spreading centers nucleated with a different mechanism.

5.2.2. Three Types of Spreading Center Nucleation

[29] The first (eastern) ridge portion nucleated in an ancient oceanic lithosphere, between the eastern edges of Arabia and Africa to the OFZ (Figure 12, stage An6) [*Stein and Cochran*, 1985]. The age of the oceanic lithosphere is poorly constrained and could be Late Jurassic-Early Cretaceous like the northern Somali Basin [*Bunce et al.*, 1967; *Cochran*, 1988] and like ophiolites emplaced on the Oman margin [*Beurrier*, 1987; *Smewing et al.*, 1991; *Peters and Mercolli*, 1998; *Fournier et al.*, 2006] or Late Cretaceous or younger from correlations of seismic profiles with the DSDP drillings [*Mountain and Prell*, 1990; *Edwards et al.*, 2000]. The western limit of this ridge portion corresponds approximately to the east African continent/ocean boundary.

[30] The second (central) ridge portion composed of six segments was emplaced westward up to the Alula-Fartak transform fault (Figure 12, stage An5D). In this area, as noticed by *McKenzie et al.* [1970], Socotra does not fit against Arabia when the Gulf of Aden is closed. More largely, a variable amount of extension is observed along the Gulf of Aden when it is closed (i.e., at the onset of seafloor accretion). In the eastern Gulf of Aden, an important gap remains between the 500 m isobaths on each side of the Gulf, whereas in the western Gulf of Aden the contours are
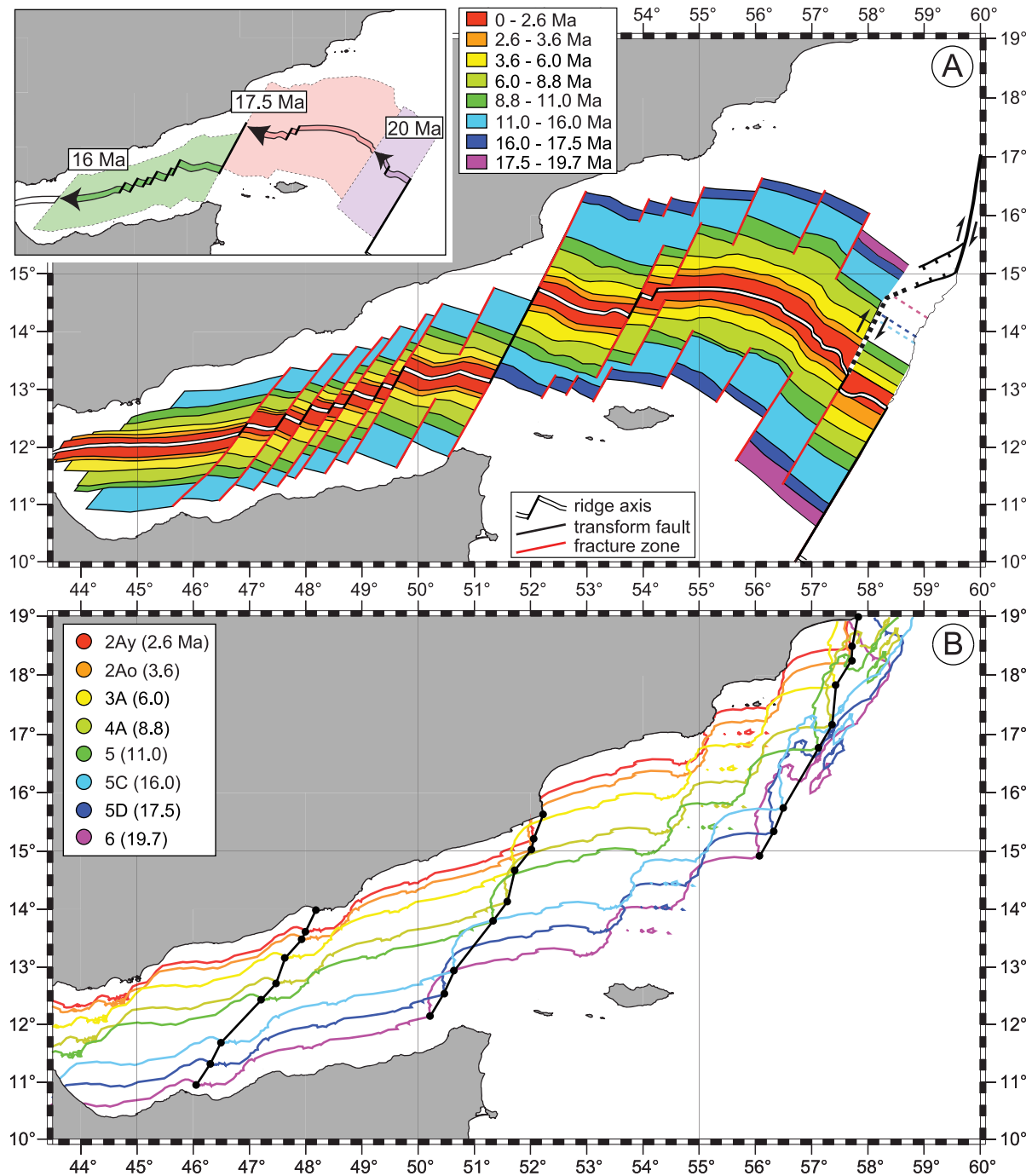
Figure 11

Figure 11. (a) Age of the oceanic crust in the Gulf of Aden inferred from magnetic isochrons. The present-day axis of the Sheba Ridge accurately mapped from bathymetric data is superimposed on magnetic data. Inset shows the three main portions of the Sheba Ridge emplaced at chrons 6 (19.7 Ma), 5D (17.5 Ma), and 5C (16.0 Ma). (b) Reconstruction of the Arabia coastline with respect to Somalia at each anomaly time and trajectories of three points through time.

closely superimposed (Figure 12; stage An6). The gap in the eastern part of the Gulf corresponds to crust that does not bear any magnetic signal, identified as highly stretched continental crust on seismic profiles [*d'Acremont et al.*, 2005]. There, spreading segments nucleated in stretched continental crust following approximately the line of the

syn-rift grabens. East of Socotra transform fault, spreading center nucleation occurred in the southern part of the Gulf, close to Socotra, separating two conjugate continental margins asymmetric in map view, a ~100 km-wide margin to the north and ~30 km-wide to the south (Figure 12, stage An5D). Seismic profiles across these margins show that they are

Table 2. Stages Poles Attached to the Somalia Plate

Anomaly	Time Interval (Ma)	Latitude (°N)	Longitude (°E)	ω (deg)
0–2Ay	0–2.58	23.67	22.21	0.939
2Ay–2Ao	2.58–3.60	17.58	36.63	0.694
2Ao–3A	3.60–6.03	33.88	18.57	0.797
3A–4A	6.03–8.77	18.05	30.82	1.599
4A–5	8.77–11.04	30.88	21.10	0.764
5–5C	11.04–15.97	30.36	22.73	2.125
5C–5D	15.97–17.53	27.05	−11.80	0.508
5D–6	17.53–19.72	30.96	4.11	0.571

asymmetric in cross section too [*Fournier et al.*, 2007]. The northern margin extends over a distance of about 100 km from the coastline (Al Hallaniyah islands) and is dominated by conjugate normal faults delimiting horsts and grabens, i.e., by pure shear extension. In contrast, the southern margin is steep, narrow (~30 km), marked by one major, northward dipping normal fault, and was formed in simple shear regime. The same type of asymmetry is observed along the segment located immediately west of Socotra transform fault [*d'Acremont et al.*, 2005].

[31] The mode of emplacement of the third (western) ridge portion was again different. The spreading center propagated very rapidly (>45 cm yr^{-1}) crosscuting the existing WNW-ESE trending horsts and grabens formed by previous continental extension (Figure 12, stage An5C). The continental margins in this part of the Gulf are very narrow and attest of a very small amount of extension. The westward decrease of continental extension in the Gulf of Aden is in contradiction with the propagating rift model for continental breakup proposed by *Vink* [1982], in which the amount of extension in the continental lithosphere increases in the direction of rift propagation, as observed for example in the South China Sea [*Huchon et al.*, 2001].

5.3. Evolution of the Sheba Ridge Segmentation

[32] The magnetic anomalies mapped on the flanks of the ridge record a succession of events which occurred at the spreading axis. The isochrons were reassembled using finite rotation poles to restore the former plate boundary configuration and define the changes in axial geometry through time (Figure 12).

[33] In the eastern part of the Gulf of Aden, the number of ridge segments has varied a lot during the opening. Between the Owen and Alula-Fartak transform faults, the ridge was initially (from Chron 5D to 5C) made up of eight segments separated by seven transform faults, two right-stepping transforms to the east and five left-stepping to the west. Between chrons 5C and 5, three transform faults were abandoned and two new ones appeared, so that at Chron 5, the ridge was made up of seven segments separated by six transform faults.

The most important change occurred between Chron 4A (8.8 Ma) and Chron 3A (6.0 Ma) with the deactivation of three transform faults out of six and the evolution of a ridge from seven to four segments with a 370 km-long central segment. These changes in geometry of the ridge were accommodated by ridge jumps. Most of the observed segments do not seem to have significantly changed in length through time.

[34] To the west of the Alula-Fartak transform fault, the geometry of the axis remained stable during most of the opening of the Gulf of Aden. The axis geometry in this part of the Gulf is mainly inferred from multibeam and satellite-derived bathymetric data, complemented by magnetic data. Between 47° and 50°E, the ridge axis is offset by seven left-stepping transform faults (offset < 50 km). One transform fault at the latitude of 50°E, which formed at the inception of spreading at Chron 5C, was essentially eliminated between chrons 3A and 2Ao.

[35] These reconstructions reveal several reorganizations of the segmentation of the spreading axis, including a major change of the axial configuration of the eastern Sheba Ridge between chrons 4A and 3A.

5.4. Asymmetry of Seafloor Spreading

[36] To first order, spreading along the Sheba Ridge is asymmetric and the sense of asymmetry changes along-strike along each ridge portion, as often observed along mid-ocean ridges [e.g., *Müller et al.*, 1998]. Along the western (west of the Alula-Fartak transform fault) and eastern ridge portions, spreading is faster on average on the southern flank than on the northern one. Along the central ridge portion, the spreading rate is higher to the north than to the south. There is however a great variability depending on the segments and the time period. For instance, between chrons 5C and 5 (16.0–11.0 Ma), the spreading rate along the central ridge portion (between the Alula-Fartak and Socotra transform faults) is more than twice higher on the northern flank than on the southern one. Further east, spreading is symmetric and asymmetry is opposite along the two easternmost segments.

5.5. Comparison With Geodetic Poles

[37] Recent geodetic models predict full rates on the Sheba Ridge ranging from 1.7 cm yr^{-1} [*Vigny et al.*, 2006] to 2.1 cm yr^{-1} [*Reilinger et al.*, 2006] close to the Alula-Fartak transform fault, where our model predicts a rate of 2.0 cm yr^{-1} (Figure 10). Several geodetic studies suggest that the present-day spreading rates in the Gulf of Aden and the Red Sea may be 15–20% lower than those measured from magnetic anomalies and spreading directions rotated 6–7° counterclockwise with respect to other models [*Vigny et al.*, 2006; *Nocquet et al.*, 2006; *Le Beon et al.*, 2008].

Figure 12. Reconstruction of the opening of the Gulf of Aden at each anomaly time illustrating the westward propagation of the Sheba Ridge toward the Afar mantle plume and the evolution of the axial segmentation. Seafloor spreading between the Arabia and Somalia plates started ~20 Myr ago, shortly before anomaly 6 (19.7 Ma), the oldest magnetic anomaly recognized in the Gulf of Aden. The syn-rift structures are shown for the three stages of ridge propagation (chrons 6, 5D, and 5C). The ridge propagation in most of Gulf of Aden was completed at Chron 5C (16.0 Ma). The ridge propagated extremely fast at a mean rate of 350 km Myr^{-1}. The number of ridge segments has varied with time, with a major change in geometry of the eastern Sheba Ridge between chrons 4A and 3A.
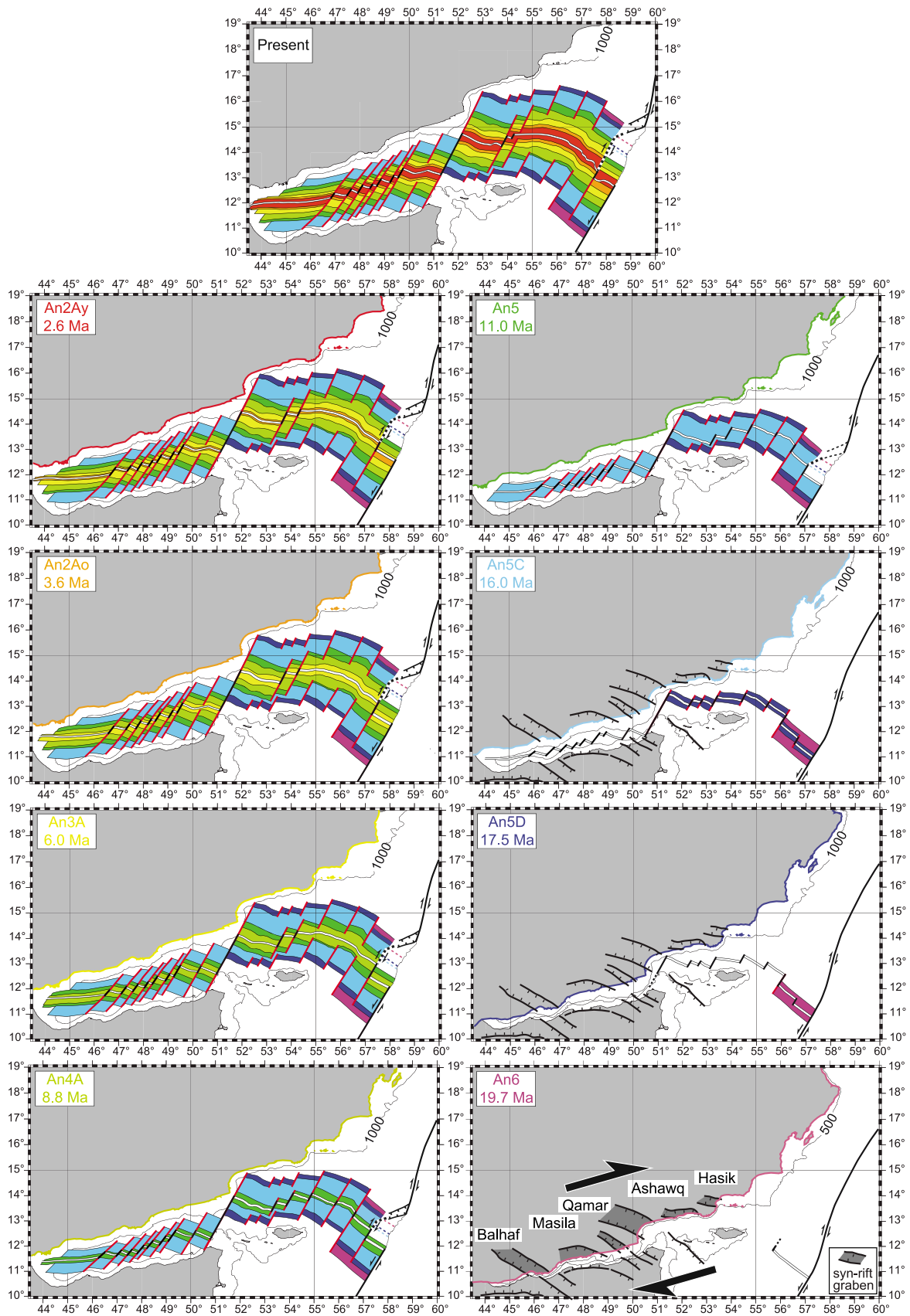
Figure 12

Figure 12

Table 3. Azimuths of Transform Faults and Slip Vectors Along the Sheba Ridge

Latitude (°N)	Longitude (°E)	Azimuth[a] (deg)	Type[b]	Source
12.58	48.00	30.5	TF	this study
13.33	49.63	27	TF	this study
13.52	51.32	26	SV	CMT, 24 Jun 2000
13.66	51.06	27	SV	CMT, 14 Sep 1990
13.67	51.44	27	SV	CMT, 30 Dec 2006
13.80	51.58	25	SV	CMT, 4 Mar 2004
13.94	51.53	22	SV	CMT, 15 Dec 2006
13.96	51.52	29	SV	CMT, 16 Jul 1988
14.00	51.58	23	SV	CMT, 26 Apr 2008
14.00	51.83	24.5	TF	this study
14.03	51.59	23	SV	CMT, 15 Jun 2001
14.07	51.64	23	SV	CMT, 22 Dec 1979
14.27	51.82	28	SV	CMT, 28 Jan 1984
14.38	51.74	22	SV	CMT, 26 Aug 2001
14.42	51.81	23	SV	CMT, 11 Oct 2003
14.43	51.72	24	SV	CMT, 7 Jun 1997
14.45	51.83	24	SV	CMT, 1 Sep 2002
14.50	53.83	23	TF	this study
14.57	51.96	24	SV	CMT, 26 Aug 2005
14.57	53.70	22	SV	CMT, 8 Apr 2007
14.58	51.84	25	SV	CMT, 2 Sep 2002
14.69	53.65	20	SV	CMT, 1 Oct 1998
14.76	53.76	23	SV	CMT, 24 May 2003
14.81	53.77	23	SV	CMT, 8 Jul 1979
14.94	53.58	24	SV	CMT, 9 Nov 1993

[a]In degrees clockwise from north.
[b]TF is transform fault, SV is slip vector.

[38] We compared "geologic" rotation poles obtained from magnetic data and "geodetic" poles obtained from GPS data for the prediction of rates and directions. For the rates, the slow and gradual decrease from 10 to 2.6 Ma (Chron 2Ay) evidenced by magnetic data (Figure 10) is not in line with the 15–20% slowing down of the Arabia-Somalia plate motion suggested from the comparison of GPS velocities [*Calais et al.*, 2003; *Vigny et al.*, 2006; *Le Beon et al.*, 2008] with the 3.1 Ma average velocities of NUVEl-1A geological model [*DeMets et al.*, 1990, 1994; *Chu and Gordon*, 1998]. Our data show that deceleration, if any, should have occurred during the last 2.6 Ma. A crucial issue is the potential effect of outward displacement of magnetic anomalies as described and modeled by *DeMets and Wilson* [2008]. In their analysis, they quote total outward displacement of 3–4.5 km (1.5–2.25 km for each flank) for the Carlsberg Ridge, with an average of 3.3 km. No such estimate is available for the Sheba Ridge, but using the same 3.3 km value would slightly change our spreading rate estimation for the youngest chron (relative distance between older chrons would not be affected if the outward displacement is constant through time). Correcting for the outward displacement would actually lower the full opening rate by about 1 mm yr⁻¹ for Chron C2An.1y. If the outward displacement for the Sheba Ridge is closer to the global average (2.2 ± 0.3 km) [*DeMets and Wilson*, 2008], then the bias in spreading rate would be less than 1 mm yr⁻¹, which is clearly within the errors of our model (see 95% error bars in Figure 10). On the other hand, the GPS estimates are not consistent with each other, which suggests that their uncertainties are still greater than ±1 or ±2 mm yr⁻¹. The geologic and GPS data are therefore compatible with constant seafloor spreading rates in the Gulf of Aden for the past 5 Myr, although a limited slow down cannot be ruled out.

[39] In terms of directions, geodetic poles obtained from GPS regional surveys based on numerous geodetic sites [*Vigny et al.*, 2006; *Reilinger et al.*, 2006] and geologic poles (NUVEL-1A and Chron 2Ay from this study) are tested with the azimuths of transform faults and slip vectors of strike-slip earthquakes along the Sheba Ridge (Figure 11b and Table 3). Theoretically, great circles perpendicular to transform faults and earthquake slip vectors should intersect near the rotation pole [*Morgan*, 1968]. The geologic poles correctly predict the direction of motion along the plate boundary, whereas the geodetic poles predict a more northward direction (Figure 9b).

6. Conclusion

[40] Comprehensive examination of marine magnetic data in the Gulf of Aden reveals the detailed history of seafloor spreading between the Arabia and Somalia plates from the AOC triple junction to the Afar triple junction for the past 20 Myr. The main results of this study are as follows:

[41] 1. Seafloor spreading in the Gulf of Aden started shortly before Chron 6 (19.7 Ma), after a phase of extension of the continental lithosphere between 30 and 20 Ma. According to the reconstruction of the Gulf at the onset of seafloor accretion, rifting proceeded at a very slow rate and was accommodated by a series of grabens arranged en échelon within a 200 km-wide dextral shear zone.

[42] 2. Initiation of seafloor spreading was a sudden event associated with a relatively high spreading rate (about 3 cm yr⁻¹) and a rapid propagation of the spreading ridge across the rift system.

[43] 3. The seafloor-spreading axis propagated westward in the Gulf of Aden and three stages of propagation are identified from magnetic data. The Sheba Ridge started from the Owen fracture zone about 20 Ma, crossed the East-African continent-ocean boundary at about 18 Ma, and stepped across the Alula-Fartak transform fault at approximately 17 Ma to reach the western end of the Gulf (45°E) by 16 Ma. The ridge propagation proceeded at an extremely fast average rate of 35 cm yr⁻¹ in response to the Arabia-Somalia plate rotation about an almost stationary pole. The three stages of propagation correspond to three types of spreading center nucleation, including nucleation in ancient oceanic lithosphere, nucleation in a highly stretched continental lithosphere, and nucleation crosscutting preexisting horsts and grabens formed during the rifting phase.

[44] 4. The high-resolution model for Arabia-Somalia plate kinematics indicates that seafloor spreading rates slowed down rapidly by 30% from 17 Ma to 10 Ma and then slowly by 10% during the last 10 Myr. Similar decelerations of seafloor spreading rates between 20 and 10 Ma with a change around 10 Ma are reported along the Carlsberg Ridge (India-Somalia motion) and the southern Central Indian Ridge (Capricorn-Somalia motion) [*DeMets et al.*, 2005; *Merkouriev and DeMets*, 2006], suggesting that the motions of the Arabian, Indian and Capricorn plates are strongly coupled. A reappraisal of the Arabia-India plate kinematics with the new Arabia-Somalia plate motion model is necessary.

[45] 5. The evolution of the AOC triple junction was marked by a change of geometry of the Arabia-India plate boundary around 10 Ma and the formation of the Beautemps-Beaupré Basin. A small part of the Arabian plate was then transferred to the Indian plate. This change of geometry was coeval with a regional kinematic reorganization corresponding to the onset of intraplate deformation in the India-Australia plate and a change of kinematics along the Sheba, Carlsberg, and southern Central Indian ridges.

[46] 6. The reconstructions of the spreading axis at each anomaly time reveal the complex history of the ridge segmentation. It involves several reorganizations of the axial geometry, including a major change of configuration of the eastern Sheba Ridge between chrons 4A and 3A. Moreover, seafloor spreading is asymmetric and the sense of asymmetry changes along-strike.

[47] 7. Long-term (averaged over the last 2.6 Ma) and short-term (obtained from geodetic solutions) opening rates agree within 2 mm yr^{-1}. Taking into account uncertainties in both techniques, and in particular the unresolved outward displacement of the magnetic chrons for the Sheba Ridge, we cannot rule out a slightly lower opening rate for the recent period, as suggested by geodesy.

References

Abbate, E. P., P. Bruni, and M. Sagri (1993), Tertiary basins in the northern Somalia continental margin: Their structural significance in the Gulf of Aden rift system, in *Geoscientific Research in Northeast Africa*, edited by U. Thorweihe and H. Schandelmeier, pp. 291–294, A. A. Balkema, Brookfield, Vt.

Abbate, E. P., M. L. Balestrieri, and G. Bigazzi (2001), Uplifted rift-shoulder of the Gulf of Aden in northwestern Somalia: Palinspastic reconstructions supported by apatite fission-track data, in *Peri-Tethys Memoir 6: Peri-Tethyan Rift/Wrench Basins and Passive Margins*, edited by P. A. Ziegler et al., *Mem. Mus. Natl. Hist. Nat.*, 186, 629–640.

Agard, P., J. Omrani, L. Jolivet, and F. Mouthereau (2005), Convergence history across Zagros (Iran): Constraints from collisional and earlier deformation, *Int. J. Earth Sci.*, 94 401–419, doi:10.1007/s00531-005-0481-4.

Audin, L., I. Manighetti, P. Tapponnier, F. Métivier, E. Jacques, and P. Huchon (2001), Fault propagation and climatic control of sedimentation on the Goubbet Rift Floor: Insights from the Tadjouraden cruise in the western Gulf of Aden, *Geophys. J. Int.*, 144, 391–414, doi:10.1046/j.0956-540x.2000.01322.x.

Audin, L., et al. (2004), Palaeomagnetism and K-Ar and ^{40}Ar/^{39}Ar ages in the Ali Sabieh area (Republic of Djibouti and Ethiopia): Constraints on the mechanism of Aden ridge propagation into southeastern Afar during the last 10 Myr, *Geophys. J. Int.*, 158, 327–345, doi:10.1111/j.1365-246X.2004.02286.x.

Baker, J., L. Snee, and M. Menzies (1996), A brief Oligocene period of flood volcanism in Yemen: Implications for the duration and rate of continental flood volcanism at the Afro-Arabian triple junction, *Earth Planet. Sci. Lett.*, 138, 39–55, doi:10.1016/0012-821X(95)00229-6.

Bellahsen, N., C. Faccenna, F. Funiciello, J.-M. Daniel, and L. Jolivet (2003), Why did Arabia separate from Africa? Insights from 3-D laboratory experiments, *Earth Planet. Sci. Lett.*, 216, 365–381, doi:10.1016/S0012-821X(03)00516-8.

Bellahsen, N., M. Fournier, E. d'Acremont, S. Leroy, and J.-M. Daniel (2006), Fault reactivation and rift localization: The northeastern Gulf of Aden margin, *Tectonics*, 25, TC1007, doi:10.1029/2004TC001626.

Beurrier, M. (1987), Géologie de la nappe ophiolitique de Semail dans les parties orientales et centrales de l'Oman, 406 pp., Thèse Doc. Etat, Univ. Paris 6, Paris.

Beydoun, Z. R. (1964), The stratigraphy and structure of the eastern Aden Protectorate, *Overseas Geol. Miner. Resour.*, 5, 107 pp.

Beydoun, Z. R. (1970), Southern Arabia and northern Somalia: Comparative geology, *Philos. Trans. R. Soc. London, Ser. A*, 267, 267–292, doi:10.1098/rsta.1970.0036.

Beydoun, Z. R. (1982), The Gulf of Aden and northwest Arabian Sea, in *The Oceans Basins and Margins*, vol. 6, *The Indian Ocean*, edited by A. E. M. Nairn and F. G. Stehli, pp. 253–313, Plenum, New York.

Beydoun, Z. R., and M. R. Bichan (1969), The Geology of Socotra Island, Gulf of Aden, *Q. J. Geol. Soc. Am.*, 91, 699–706.

Birse, A. C. R., W. F. Bott, J. Morrison, and M. A. Samuel (1997), The Mesozoic and Tertiary tectonic evolution of the Socotra area, eastern Gulf of Aden, Yemen, *Mar. Pet. Geol.*, 14, 675–683, doi:10.1016/S0264-8172(96)00043-8.

Bosworth, W., P. Huchon, and K. McClay (2005), The Red Sea and Gulf of Aden basins, *J. Afr. Earth Sci.*, 43, 334–378, doi:10.1016/j.jafrearsci.2005.07.020.

Bott, M. H. P. (1982), The mechanism of continental splitting, *Tectonophysics*, 81, 301–309, doi:10.1016/0040-1951(82)90134-2.

Bott, W. F., B. A. Smith, G. Oakes, A. H. Sikander, and A. I. Ibraham (1992), The tectonic framework and regional hydrocarbon prospectivity of the Gulf of Aden, *J. Pet. Geol.*, 15, 211–243, doi:10.1111/j.1747-5457.1992.tb00963.x.

Brannan, J., K. D. Gerdes, and I. R. Newth (1997), Tectono-stratigraphic development of the Qamar basin, Eastern Yemen, *Mar. Pet. Geol.*, 14, 701–730, doi:10.1016/S0264-8172(96)00048-7.

Bunce, E. T., M. G. Langseth, R. L. Chase, and M. Ewing (1967), Structure of the western Somali Basin, *J. Geophys. Res.*, 72, 25477–2555, doi:10.1029/JZ072i010p02547.

Burke, K. (1996), The African Plate, *S. Afr. J. Geol.*, 99, 341–409.

Calais, E., C. DeMets, and J.-M. Nocquet (2003), Evidence for a post-3.16 Ma change in Nubia-Eurasia-North America plate motions?, *Earth Planet. Sci. Lett.*, 216, 81–92, doi:10.1016/S0012-821X(03)00482-5.

Cande, S. C., and D. V. Kent (1992), A new geomagnetic polarity time scale for the Late Cretaceous and Cenozoic, *J. Geophys. Res.*, 97, 13,917–13,951, doi:10.1029/92JB01202.

Cande, S. C., and D. V. Kent (1995), Revised calibration of the geomagnetic polarity timescale for the Late Cretaceous and Cenozoic, *J. Geophys. Res.*, 100, 6093–6095, doi:10.1029/94JB03098.

Cann, J. R., D. K. Blackman, D. K. Smith, E. McAllister, B. Janssen, S. Mello, E. Avgerinos, A. R. Pascoe, and J. Escartin (1997), Corrugated slip surfaces formed at ridge-transform intersections on the Mid-Atlantic Ridge, *Nature*, 385, 329–332, doi:10.1038/385329a0.

Cannat, M., D. Sauter, V. Mendel, E. Ruellan, K. Okino, J. Escartin, V. Combier, and M. Baala (2006), Modes of sea floor generation at a melt-poor ultraslow-spreading ridge, *Geology*, 34, 605–608, doi:10.1130/G22486.1.

Chamot-Rooke, N., V. Renard, and X. Le Pichon (1987), Magnetic anomalies in the Shikoku Basin: A new interpretation, *Earth Planet. Sci. Lett.*, 83, 214–228, doi:10.1016/0012-821X(87)90067-7.

Chamot-Rooke, N., F. Jestin, and B. De Voogd, and the Phèdre Working Group (1993), Intraplate shortening in the central Indian Ocean determined from 2100-km-long north-south deep seismic reflection profile, *Geology*, 21, 1043–1046, doi:10.1130/0091-7613(1993)021<1043:ISITCI>2.3.CO;2.

Chase, C. G. (1978), Plate kinematics: The Americas, East Africa and the rest of the world, *Earth Planet. Sci. Lett.*, 37, 355–368, doi:10.1016/0012-821X(78)90051-1.

Chaubey, A., et al. (1998), Early Tertiary seafloor spreading magnetic anomalies and paleopropagators in the northern Arabian Sea, *Earth Planet. Sci. Lett.*, 154, 41– 53, doi:10.1016/S0012-821X(97)00178-7.

Chaubey, A. K., J. Dyment, G. C. Bhattacharya, J.-Y. Royer, K. Srinivas, and V. Yatheesh (2002), Paleogene magnetic isochrons and paleo-propagators in the Arabian and eastern Somali basins, northwest Indian Ocean, in *The Tectonic and Climatic Evolution of the Arabian Sea Region*, edited by P. Clift et al., *Geol. Soc. Spec. Publ.*, 195, 71–85.

Choukroune, P., B. Auvray, J. Francheteau, J.-C. Lépine, F. Arthaud, J.-P. Brun, J.-M. Auzende, B. Sichler, and Y. Khobar (1986), Tectonics of the westernmost Gulf of Aden and the Gulf of Tadjoura from submersible observations, *Nature*, 319, 396–399, doi:10.1038/319396a0.

Choukroune, P., J. Francheteau, B. Auvray, J.-M. Auzende, J.-P. Brun, B. Sichler, F. Arthaud, and J.-C. Lépine (1988), Tectonics of an incipient oceanic rift, *Mar. Geophys. Res.*, 9, 147–163, doi:10.1007/BF00369246.

Chu, D., and R. Gordon (1998), Current plate motions across the Red Sea, *Geophys. J. Int.*, 135, 313–328, doi:10.1046/j.1365-246X.1998.00658.x.

Cochran, J. R. (1981), The Gulf of Aden: Structure and evolution of a young ocean basin and continental margin, *J. Geophys. Res.*, *86*, 263–287, doi:10.1029/JB086iB01p00263.

Cochran, J. R. (1982), The magnetic quiet zone in the eastern of the Gulf of Aden: Implications for the early development of the continental margin, *Geophys. J. R. Astron. Soc.*, *68*, 171–201.

Cochran, J. R. (1988), Somali Basin, Chain Ridge, and origin of the northern Somali Basin gravity and geoid low, *J. Geophys. Res.*, *93*, 11,985–12,008, doi:10.1029/JB093iB10p11985.

Cochran, J. R. (1990), Himalayan uplift, sea level, and the record of Bengal Fan sedimentation at the ODP LEG 116 Sites, *Proc. Ocean Drill. Program, Sci. Results*, *116*, 397–414.

Cochran, J. R., and G. D. Karner (2007), Constraints on the deformation and rupturing of continental lithosphere of the Red Sea: The transition from rifting to drifting, in *The Origin and Evolution of the Caribbean Plate*, edited by K. H. James, M. A. Lorente, and J. L. Pindell, *Geol. Soc. Spec. Publ.*, *282*, 265–289, doi:10.1144/SP282.13.

Collier, J. S., V. Sansom, O. Ishizuka, R. N. Taylor, T. A. Minshull, and R. B. Whitmarsh (2008), Age of Seychelles-India break-up, *Earth Planet. Sci. Lett.*, *272*, 264–277, doi:10.1016/j.epsl.2008.04.045.

Corti, G. (2008), Control of rift obliquity on the evolution and segmentation of the main Ethiopian rift, *Nat. Geosci.*, *1*, 258–262, doi:10.1038/ngeo160.

Courtillot, V. (1980), Opening of the Gulf of Aden and Afar by progressive tearing, *Phys. Earth Planet. Inter.*, *21*, 343–350, doi:10.1016/0031-9201(80)90137-5.

Courtillot, V. (1982), Propagating rifts and continental breakup, *Tectonics*, *1*, 239–256, doi:10.1029/TC001i003p00239.

Courtillot, V., and G. E. Vink (1983), How continents break up, *Sci. Am.*, *249*, 40–47.

Courtillot, V., C. Jaupart, I. Manighetti, P. Tapponnier, and J. Besse (1999), On causal links between flood basalts and continental breakup, *Earth Planet. Sci. Lett.*, *166*, 177–195, doi:10.1016/S0012-821X(98)00282-9.

d'Acremont, E., S. Leroy, M.-O. Beslier, N. Bellahsen, M. Fournier, C. Robin, M. Maia, and P. Gente (2005), Structure and evolution of the eastern Gulf of Aden conjugate margins from seismic reflection data, *Geophys. J. Int.*, *160*, 869–890, doi:10.1111/j.1365-246X.2005.02524.x.

d'Acremont, E., S. Leroy, M. Maia, P. Patriat, M.-O. Beslier, N. Bellahsen, M. Fournier, and P. Gente (2006), Structure and evolution of the eastern Gulf of Aden: Insights from magnetic and gravity data (Encens Sheba Cruise), *Geophys. J. Int.*, *165*, 786–803, doi:10.1111/j.1365-246X.2006.02950.x.

Dauteuil, O., P. Huchon, F. Quemeneur, and T. Souriot (2001), Propagation of an oblique spreading centre: The western Gulf of Aden, *Tectonophysics*, *332*, 423–442, doi:10.1016/S0040-1951(00)00295-X.

Delescluse, M., and N. Chamot-Rooke (2007), Instantaneous deformation and kinematics of the India-Australia Plate, *Geophys. J. Int.*, *168*, 818–842, doi:10.1111/j.1365-246X.2006.03181.x.

Delescluse, M., L. Montési, and N. Chamot-Rooke (2008), Fault reactivation and selective abandonment in the oceanic lithosphere, *Geophys. Res. Lett.*, *35*, L16312, doi:10.1029/2008GL035066.

DeMets, C. (2008), Arabia's slow dance with India, *Nat. Geosci.*, *1*, 10–11, doi:10.1038/ngeo.2007.56.

DeMets, C., and D. S. Wilson (2008), Toward a minimum change model for recent plate motions: Calibrating seafloor spreading rates for outward displacement, *Geophys. J. Int.*, *174*, 825–841, doi:10.1111/j.1365-246X.2008.03836.x.

DeMets, C., R. G. Gordon, D. F. Argus, and S. Stein (1990), Current plate motions, *Geophys. J. Int.*, *101*, 425–478, doi:10.1111/j.1365-246X.1990.tb06579.x.

DeMets, C., R. G. Gordon, D. F. Argus, and S. Stein (1994), Effect of recent revisions to the geomagnetic reversal time scale on estimates of current plate motions, *Geophys. Res. Lett.*, *21*, 2191–2194, doi:10.1029/94GL02118.

DeMets, C., R. G. Gordon, and J.-Y. Royer (2005), Motion between the Indian, Capricorn, and Somalian plates since 20 Ma: Implications for the timing and magnitude of distributed deformation in the equatorial Indian Ocean, *Geophys. J. Int.*, *161*, 445–468, doi:10.1111/j.1365-246X.2005.02598.x.

Dercourt, J., L. E. Ricou, and B. Vrielynck (1993), *Atlas Tethys Palaeoenvironmental Maps*, 307 pp., Gauthier-Villars, Paris.

Dyment, J. (1998), Evolution of the Carlsberg ridge between 60 and 45 Ma: Ridge propagation, spreading asymmetry, and the Deccan-reunion hotspot, *J. Geophys. Res.*, *103*, 24,067–24,084, doi:10.1029/98JB01759.

Ebinger, C. J., and N. H. Sleep (1998), Cenozoic magmatism throughout east African resulting from impact of a single plume, *Nature*, *395*, 788–791, doi:10.1038/27417.

Ebinger, C. J., D. Keir, A. Ayele, E. Calais, T. J. Wright, M. Belachew, J. O. S. Hammond, E. Campbell, and W. R. Buck (2008), Capturing magma intrusion and faulting processes during continental rupture: Seismicity of the Dabbahu (Afar) rift, *Geophys. J. Int.*, *174*, 1138–1152, doi:10.1111/j.1365-246X.2008.03877.x.

Edwards, R. A., T. A. Minshull, and R. S. White (2000), Extension across the Indian-Arabian plate boundary: The Murray Ridge, *Geophys. J. Int.*, *142*, 461–477, doi:10.1046/j.1365-246x.2000.00163.x.

Edwards, R. A., T. A. Minshull, E. R. Flueh, and C. Kopp (2008), Dalrymple Trough: An active oblique-slip ocean-continent boundary in the northwest Indian Ocean, *Earth Planet. Sci. Lett.*, *272*, 437–445, doi:10.1016/j.epsl.2008.05.007.

Ellouz-Zimmermann, N., E. Deville, C. Müller, S. Lallemant, A. Subhani, and A. Tabreez (2007a), *Impact of sedimentation on convergent margin tectonics: Example of the Makran accretionary prism (Pakistan)*, in *Thrust Belts and Foreland Basins: From Fold Kinematics to Hydrocarbon System*, edited by O. Lacombe et al., pp. 327–350, doi:10.1007/978-3-540-69426-7_17, Springer, Berlin.

Ellouz-Zimmermann, N., et al. (2007b), Offshore frontal part of the Makran Accretionary prism: The Chamak survey (Pakistan), in *Thrust Belts and Foreland Basins: From Fold Kinematics to Hydrocarbon System*, edited by O. Lacombe et al., pp. 351–366, doi:10.1007/978-3-540-69426-7_18, Springer, Berlin.

Escartin, J., D. K. Smith, J. R. Cann, H. Schouten, C. H. Langmuir, and S. Escrig (2008), Central role of detachment faults in accretion of slow spreading oceanic lithosphere, *Nature*, *455*, 790–794, doi:10.1038/nature07333.

Ewing, M., and B. C. Heezen (1960), Continuity of mid-oceanic ridge and rift valley in the southwestern Indian Ocean confirmed, *Science*, *131*, 1677–1679, doi:10.1126/science.131.3414.1677.

Fantozzi, P. L. (1996), Transition from continental to oceanic rifting in the Gulf of Aden: Structural evidence from field mapping in Somalia and Yemen, *Tectonophysics*, *259*, 285–311, doi:10.1016/0040-1951(95)00208-1.

Fantozzi, P. L., and M. Ali Kassim (2002), Geological mapping in northeastern Somalia (Midjiurtinia region): Field evidence of the structural and paleogeographic evolution of the northern margin of the Somalian plate, *J. Afr. Earth Sci.*, *34*, 21–55, doi:10.1016/S0899-5362(01)00100-2.

Fantozzi, P. L., and M. Sgavetti (1998), Tectonic and sedimentary evolution of the eastern Gulf of Aden continental margins: New structural and stratigraphic data from Somalia and Yemen, in *Sedimentation and Tectonics of Rift Basins: Red Sea-Gulf of Aden*, edited by B. H. Purser and D. W. J. Bosence, pp. 56–76, Chapman and Hall, London.

Farquharson, W. I. (1936), *1933–34 Topography*, John Murray Expedition, Br. Mus. of Nat. Hist., London.

Fournier, M., and C. Petit (2007), Oblique rifting at oceanic ridges: Relationship between spreading and stretching directions from earthquake focal mechanisms, *J. Struct. Geol.*, *29*, doi:10.1016/j.jsg.2006.07.017.

Fournier, M., P. Patriat, and S. Leroy (2001), Reappraisal of the Arabia-India-Somalia triple junction kinematics, *Earth Planet. Sci. Lett.*, *189*, 103–114, doi:10.1016/S0012-821X(01)00371-5.

Fournier, M., N. Bellahsen, O. Fabbri, and Y. Gunnell (2004), Oblique rifting and segmentation of the NE Gulf of Aden passive margin, *Geochem. Geophys. Geosyst.*, *5*, Q11005, doi:10.1029/2004GC000731.

Fournier, M., C. Lepvrier, P. Razin, and L. Jolivet (2006), Late Cretaceous to Paleogene post-obduction extension and subsequent Neogene compression in the Oman Mountains, *GeoArabia*, *11*, 17–40.

Fournier, M., P. Huchon, K. Khanbari, and S. Leroy (2007), Segmentation and along-strike asymmetry of the passive margin in Socotra, eastern Gulf of Aden: Are they controlled by detachment faults?, *Geochem. Geophys. Geosyst.*, *8*, Q03007, doi:10.1029/2006GC001526.

Fournier, M., C. Petit, N. Chamot-Rooke, O. Fabbri, P. Huchon, B. Maillot, and C. Lepvrier (2008a), Do ridge-ridge-fault triple junctions exist on Earth? Evidence from the Aden-Owen-Carlsberg junction in the NW Indian Ocean, *Basin Res.*, *20*, 575–590, doi:10.1111/j.1365-2117.2008.00356.x.

Fournier, M., N. Chamot-Rooke, C. Petit, O. Fabbri, P. Huchon, B. Maillot, and C. Lepvrier (2008b), In-situ evidence for dextral active motion at the Arabia-India plate boundary, *Nat. Geosci.*, *1*, 54–58, doi:10.1038/ngeo.2007.24.

Gaedicke, G., H.-U. Schlüter, H. A. Roeser, A. Prexl, B. Schreckenberger, H. Meyer, C. Reichert, P. Clift, and S. Amjad (2002), Origin of the northern Indus Fan and Murray Ridge, northern Arabian Sea: Interpretation from seismic and magnetic imaging, *Tectonophysics*, *355*, 127–143, doi:10.1016/S0040-1951(02)00137-3.

Girdler, R. W. (1991), The Afro-Arabian rift system-an overview, *Tectonophysics*, *197*, 139–153, doi:10.1016/0040-1951(91)90038-T.

Girdler, R. W., and P. Styles (1974), Two-stage Red Sea floor spreading, *Nature*, *247*, 7–11, doi:10.1038/247007a0.

Girdler, R. W., and P. Styles (1978), Seafloor spreading in the western Gulf of Aden, *Nature*, *271*, 615–617, doi:10.1038/271615a0.

Girdler, R. W., C. Brown, D. J. N. Noy, and P. Styles (1980), A geophysical survey of the westernmost Gulf of Aden, *Philos. Trans. R. Soc. London, Ser. A*, *298*, 1–43, doi:10.1098/rsta.1980.0239.

Gordon, R. G., and C. DeMets (1989), Present-day motion along the Owen fracture zone and Dalrymple trough in the Arabian Sea, *J. Geophys. Res.*, *94*, 5560– 5570, doi:10.1029/JB094iB05p05560.

Gunnell, Y., A. Carter, C. Petit, and M. Fournier (2007), Post-rift seaward downwarping at passive margins: New insights from southern Oman using stratigraphy to constrain apatite fission-track and (U-Th)/He dating, *Geology*, *35*, 647–650, doi:10.1130/G23639A.1.

Hébert, H., C. Deplus, P. Huchon, K. Khanbari, and L. Audin (2001), Lithospheric structure of a nascent spreading ridge inferred from gravity data: The western Gulf of Aden, *J. Geophys. Res.*, *106*, 26,345–26,363, doi:10.1029/2000JB900391.

Heezen, B. C., and M. Tharp (1964), Physiographic diagram of the Indian Ocean, the Red Sea, the South China Sea, the Sulu Sea and the Celebes Sea, map, Geol. Soc. of Am., New York.

Hey, R. N. (1977), A new class of pseudofaults and their bearing on plate tectonics: A propagating rift model, *Earth Planet. Sci. Lett.*, *37*, 321–325, doi:10.1016/0012-821X(77)90177-7.

Hey, R. N., F. K. Dennebier, and W. J. Morgan (1980), Propagating rifts on mid-ocean ridges, *J. Geophys. Res.*, *85*, 3647–3658, doi:10.1029/JB085iB07p03647.

Hoffmann, C., V. Courtillot, G. Féraud, P. Rochette, G. Yirgu, E. Ketefo, and R. Pik (1997), Timing of the Ethiopian flood basalt event and implications for plume birth and global change, *Nature*, *389*, 838–841, doi:10.1038/39853.

Hubert-Ferrari, A., G. King, I. Manighetti, R. Armijo, B. Meyer, and P. Tapponnier (2003), Long-term elasticity in the continental lithosphere; modelling the Aden Ridge propagation and the Anatolian extrusion process, *Geophys. J. Int.*, *153*, 111–132, doi:10.1046/j.1365-246X.2003.01872.x.

Huchon, P., and K. Khanbari (2003), Rotation of the syn-rift stress field of the northern Gulf of Aden margin, *Yemen, Tectonophysics*, *364*, 147–166, doi:10.1016/S0040-1951(03)00056-8.

Huchon, P., T. N. H. Nguyen, and N. Chamot-Rooke (2001), Propagation of continental break-up in the southwestern South China Sea, in *Nonvolcanic Rifting of Continental Margins: A Comparison of Evidence From Land and Sea*, edited by R. C. L. Wilson et al., *Geol. Soc. Spec. Publ.*, *187*, 31–50.

Hughes, G. W., and Z. R. Beydoun (1992), The Red Sea-Gulf of Aden: Biostratigrapphy, lithostratigraphy and paleoenvironments, *J. Pet. Geol.*, *15*, 135–156, doi:10.1111/j.1747-5457.1992.tb00959.x.

Hughes, G. W., O. Varol, and Z. R. Beydoun (1991), Evidence for middle Oligocene rifting of the Gulf of Aden and for late Oligocene rifting of the southern Red Sea, *Mar. Pet. Geol.*, *8*, 354–358, doi:10.1016/0264-8172(91)90088-I.

Ildefonse, B., D. K. Blackman, B. E. John, Y. Ohara, D. J. Miller, and C. J. MacLeod (2007), Oceanic core complexes and crustal accretion at slow-spreading ridges, *Geology*, *35*, 623–626, doi:10.1130/G23531A.1.

Jacob, K. H., and R. L. Quittmeyer (1979), The Makran region of Pakistan and Iran: Trench-arc system with active plate subduction, in *Geodynamics of Pakistan*, edited by A. Farah and K. A. DeJong, pp. 305–317, Geol. Surv. of Pakistan, Quetta.

Jestin, F., P. Huchon, and J.-M. Gaulier (1994), The Somalia plate and the East African rift system: Present-day kinematics, *Geophys. J. Int.*, *116*, 637–654, doi:10.1111/j.1365-246X.1994.tb03286.x.

Joffe, S., and Z. Garfunkel (1987), Plate kinematics of the circum Red Sea—A reevaluation, *Tectonophysics*, *141*, 5–22, doi:10.1016/0040-1951(87)90171-5.

Jolivet, L., and C. Faccenna (2000), Mediterranean extension and the Africa-Eurasia collision, *Tectonics*, *19*, 1095–1106, doi:10.1029/2000TC900018.

Keranen, K., and S. L. Klemperer (2008), Discontinuous and diachronous evolution of the Main Ethiopian Rift: Implications for development of continental rifts, *Earth Planet. Sci. Lett.*, *265*, 96–111, doi:10.1016/j.epsl.2007.09.038.

Laughton, A. S. (1966a), The Gulf of Aden, *Philos. Trans. R. Soc. London, Ser. A*, *259*, 150–171, doi:10.1098/rsta.1966.0004.

Laughton, A. S. (1966b), The Gulf of Aden in relationship to the Red Sea and the Afar depression of Ethiopia, in *The World Rift System*, edited by T. N. Irvine, pp. 78–97, Geol. Surv. of Can., Ottawa.

Laughton, A. S., R. B. Whitmarsh, and M. T. Jones (1970), The evolution of the Gulf of Aden, *Philos. Trans. R. Soc. London, Ser. A*, *267*, 227–266, doi:10.1098/rsta.1970.0035.

Le Beon, M., Y. Klinger, A. Q. Amrat, A. Agnon, L. Dorbath, G. Baer, J. Ruegg, O. Charade, and O. Mayyas (2008), Slip rate and locking depth from GPS profiles across the southern Dead Sea Transform, *J. Geophys. Res.*, *113*, B11403, doi:10.1029/2007JB005280.

Le Pichon, X. (1968), Sea-floor spreading and continental drift, *J. Geophys. Res.*, *73*, 3661–3697, doi:10.1029/JB073i012p03661.

Le Pichon, X., and J. Francheteau (1978), A plate tectonic analysis of the Red Sea—Gulf of Aden area, *Tectonophysics*, *46*, 369–406, doi:10.1016/0040-1951(78)90214-7.

Lepvrier, C., M. Fournier, T. Bérard, and J. Roger (2002), Cenozoic extension in coastal Dhofar (southern Oman): Implications on the oblique rifting of the Gulf of Aden, *Tectonophysics*, *357*, 279–293, doi:10.1016/S0040-1951(02)00372-4.

Leroy, S., et al. (2004), From rifting to spreading in the eastern Gulf of Aden: A geophysical survey of a young oceanic basin from margin to margin, *Terra Nova*, *16*, 185–192, doi:10.1111/j.1365-3121.2004.00550.x.

Lourens, L., F. J. Hilgen, J. Laskar, N. J. Shackleton, and D. Wilson (2004), The Neogene Period, in *A Geologic Time Scale 2004*, edited by F. Gradstein et al., pp. 409–440, Cambridge Univ. Press, New York.

Lucazeau, F., et al. (2008), Persistent thermal activity at the eastern Gulf of Aden after continental break-up, *Nat. Geosci.*, *1*(12), 854–858, doi:10.1038/ngeo359.

Malkin, B. V., and A. I. Shemenda (1991), Mechanism of rifting: Considerations based on results of physical modelling and on geological and geophysical data, *Tectonophysics*, *199*, 193–210, doi:10.1016/0040-1951(91)90172-O.

Malod, J., L. Droz, B. Mustafa Kemal, and P. Patriat (1997), Early spreading and continental to oceanic basement transition beneath the Indus deep sea fan, NE Arabian Sea, *Mar. Geol.*, *141*, 221–235, doi:10.1016/S0025-3227(97)00074-1.

Manighetti, I., P. Tapponnier, V. Courtillot, and S. Gruszow (1997), Propagation of rifting along the Arabia-Somalia plate boundary: The gulfs of Aden and Tadjoura, *J. Geophys. Res.*, *102*, 2681–2710, doi:10.1029/96JB01185.

Manighetti, I., P. Tapponnier, P. Y. Gillot, E. Jacques, V. Courtillot, R. Armijo, J.-C. Ruegg, and G. King (1998), Propagation of rifting along the Arabia-Somalia plate boundary: Into Afar, *J. Geophys. Res.*, *103*, 4947–4974, doi:10.1029/97JB02758.

Martin, A. K. (1984), Propagating rifts: Crustal extension during continental rifting, *Tectonics*, *3*, 611–617, doi:10.1029/TC003i006p00611.

Matthews, D. H. (1963), A major fault scarp under the Arabian Sea displacing the Carlsberg Ridge near Socotra, *Nature*, *198*, 950–952, doi:10.1038/198950a0.

Matthews, D. H. (1966), The Owen fracture zone and the northern end of the Carlsberg Ridge, *Phil. Trans. R. Soc. London, Ser. A*, *259*, 172–186.

Matthews, D. H., C. Williams, and A. S. Laughton (1967), Mid-ocean ridge in the mouth of the Gulf of Aden, *Nature*, *215*, 1052–1053, doi:10.1038/2151052a0.

McKenzie, D. P., and W. J. Morgan (1969), Evolution of triple junctions, *Nature*, *224*, 125–133, doi:10.1038/224125a0.

McKenzie, D. P., and J. G. Sclater (1971), The evolution of the Indian Ocean since the Late Cretaceous, *Geophys. J. R. Astron. Soc.*, *25*, 437–528.

McKenzie, D. P., D. Davies, and P. Molnar (1970), Plate tectonics of the Red Sea and East Africa, *Nature*, *226*, 243–248, doi:10.1130/226243a0.

Menzies, M., K. Gallagher, A. Yelland, and A. J. Hurford (1997), Volcanic and nonvolcanic rifted margins of the Red Sea and Gulf of Aden: Crustal cooling and margin evolution in Yemen, *Geochim. Cosmochim. Acta*, *61*, 2511–2527, doi:10.1016/S0016-7037(97)00108-7.

Mercuriev, S., P. Patriat, and N. Sochevanova (1996), Evolution de la dorsale de Carlsberg: évidence pour une phase d'expansion très lente entre 40 et 25 Ma (A18 à A7), *Oceanol. Acta*, *19*, 1–13.

Merkouriev, S., and C. DeMets (2006), Constraints on Indian plate motion since 20 Ma from dense Russian magnetic data: Implications for Indian plate dynamics, *Geochem. Geophys. Geosyst.*, *7*, Q02002, doi:10.1029/2005GC001079.

Merkouriev, S., and C. DeMets (2008), A high-resolution model for Eurasia-North America plate kinematics since 20 Ma, *Geophys. J. Int.*, *173*, 1064–1084, doi:10.1111/j.1365-246X.2008.03761.x.

Miles, P., M. Munschy, and J. Segoufin (1998), Structure and early evolution of the Arabian Sea and East Somali Basin, *Geophys. J. Int.*, *134*, 876–888, doi:10.1046/j.1365-246x.1998.00625.x.

Minshull, T. A., R. S. White, P. J. Barton, and J. S. Collier (1992), Deformation at plate boundaries around the Gulf of Oman, *Mar. Geol.*, *104*, 265–277, doi:10.1016/0025-3227(92)90101-M.

Minshull, T. A., C. I. Lane, J. S. Collier, and R. B. Whitmarsh (2008), The relationship between rifting and magmatism in the northeastern Arabian Sea, *Nat. Geosci.*, *1*, 463–467, doi:10.1038/ngeo228.

Minster, J. B., and T. H. Jordan (1978), Present-day plate motions, *J. Geophys. Res.*, *83*, 5331–5354, doi:10.1029/JB083iB11p05331.

Morgan, J. W. (1968), Rises, trenches, great faults, and crustal blocks, *J. Geophys. Res.*, *73*, 1959–1982, doi:10.1029/JB073i006p01959.

Mountain, G. S., and W. L. Prell (1990), A multiphase plate tectonic history of the southeast continental margin of Oman, in *The Geology and Tectonics of the Oman Region*, edited by A. H. F. Robinson et al., *Geol. Soc. Spec. Publ.*, *49*, 725–743.

Müller, R. D., W. R. Roest, and J.-Y. Royer (1998), Asymmetric sea-floor spreading caused by ridge-plume interactions, *Nature*, *396*, 455–459, doi:10.1038/24850.

Nocquet, J.-M., P. Willis, and S. Garcia (2006), Plate kinematics of Nubia-Somalia using a combined DORIS and GPS solution, *J. Geod.*, *80*, 591–607, doi:10.1007/s00190-006-0078-0.

O'Reilly, W., K. Brown, P. Styles, and T. M. Bloxam (1993), A detailed geochemical and rock magnetic study of dredged basalt from the Sheba Ridge, Gulf of Aden, *Mar. Geophys. Res.*, *15*, 101–119, doi:10.1007/BF01204131.

Parson, L. M., and J. W. Hawkins (1994), Two-stage ridge propagation and the geological history of the Lau backarc basin, *Proc. Ocean Drill. Program, Sci. Results*, *135*, 819–828.

Parson, L. M., and I. C. Wright (1996), The Lau-Havre-Taupo back-arc basin: A southward-propagating, multi-stage evolution from rifting to spreading, *Tectonophysics*, *263*, 1–22, doi:10.1016/S0040-1951(96)00029-7.

Patriat, P. (1987), *Reconstitution de l'évolution du système de dorsales de l'Océan Indien par les méthodes de la cinématique des plaques*, 308 pp., Terr. des Terres Aust. et Antarct. Fr., Paris.

Patriat, P., and V. Courtillot (1984), On the stability of triple junctions and its relation to episodicity in spreading, *Tectonics*, *3*, 317–332, doi:10.1029/TC003i003p00317.

Patriat, P., and J. Segoufin (1988), Reconstruction of the Central Indian Ocean, *Tectonophysics*, *155*, 211–234, doi:10.1016/0040-1951(88)90267-3.

Patriat, P., H. Sloan, and D. Sauter (2008), From slow to ultraslow: A previously undetected event at the Southwest Indian Ridge at ca. 24 Ma, *Geology*, *36*, 207–210, doi:10.1130/G24270A.1.

Peters, T., and I. Mercolli (1998), Extremely thin oceanic crust in the Proto-Indian Ocean: Evidence from the Masirah Ophiolite, Sultanate of Oman, *J. Geophys. Res.*, *103*, 677–689, doi:10.1029/97JB02674.

Petit, C., M. Fournier, and Y. Gunnell (2007), Tectonic and climatic controls on rift escarpments: Erosion and flexural rebound of the Dhofar passive margin (Gulf of Aden, Oman), *J. Geophys. Res.*, *112*, B03406, doi:10.1029/2006JB004554.

Platel, J. P., and J. Roger (1989), Evolution géodynamique du Dhofar (Sultanat d'Oman) pendant le Crétacé et le Tertiaire en relation avec l'ouverture du golfe d'Aden, *Bull. Soc. Geol. Fr.*, *2*, 253–263.

Platel, J.-P., J. Roger, T. J. Peters, I. Mercolli, J. D. Kramers, and J. Le Métour (1992), Geological map of Salalah, Sultanate of Oman, sheet NE 40–09, scale 1:250,000, Oman Minist. of Petrol. and Mineral., Muscat.

Quittmeyer, R. C., and A. L. Kafka (1984), Constraints on plate motions in southern Pakistan and the northern Arabian Sea from the focal mechanisms of small earthquakes, *J. Geophys. Res.*, *89*, 2444–2458, doi:10.1029/JB089iB04p02444.

Radhakrishna, M., and R. C. Searle (2006), Isostatic Response of the Alula Fartak and Owen Fracture zones in the eastern Gulf of Aden and the adjoining Arabian Sea, *Geophys. J. Int.*, *165*, 62–72, doi:10.1111/j.1365-246X.2006.02886.x.

Reilinger, R., et al. (2006), GPS constraints on continental deformation in the Africa-Arabia-Eurasia continental collision zone and implications for the dynamics of plate interactions, *J. Geophys. Res.*, *111*, B05411, doi:10.1029/2005JB004051.

Rochette, P., E. Tamrat, G. Féraud, R. Pik, V. Courtillot, E. Kefeto, C. Coulon, C. Hoffmann, D. Vandamme, and E. Yirgu (1997), Magnetostratigraphy and timing of the Oligocene Ethiopian traps, *Earth Planet. Sci. Lett.*, *14*, 497–510.

Roger, J., J.-P. Platel, C. Cavelier, and C. Bourdillon-de-Grisac (1989), Données nouvelles sur la stratigraphie et l'histoire géologique du Dhofar (Sultanat d'Oman), *Bull. Soc. Geol. Fr.*, *2*, 265–277.

Rothé, J. P. (1954), La zone séismique médiane Indo-Atlantique, *Proc. R. Soc. London, Ser. A*, *222*, 387–397.

Royer, J.-Y., A. K. Chaubey, J. Dyment, G. C. Bhattacharya, K. Srinivas, V. Yatheesh, and T. Ramprasad (2002), Paleogene plate tectonic evolution of the Arabian and eastern Somali basins, in *The Tectonic and Climatic Evolution of the Arabian Sea Region*, edited by P. Clift et al., *Geol. Soc. Spec. Publ.*, *195*, 7–23.

Sahota, G. (1990), Geophysical investigations of the Gulf of Aden Continental Margins: Geodynamic implications for the Development of the Afro-Arabian Rift System, Ph.D. thesis, Univ. College, Swansea, U. K.

Samuel, M. A., N. A. Harbury, W. F. Bott, and A. M. Thabet (1997), Field observations from the Socotran Platform: Their interpretation and correlation to southern Oman, *Mar. Pet. Geol.*, *14*, 661–672, doi:10.1016/S0264-8172(96)00033-5.

Sandwell, D. T., and W. H. F. Smith (1997), Marine gravity anomaly from Geosat and ERS-1 satellite altimetry, *J. Geophys. Res.*, *102*, 10,039–10,054, doi:10.1029/96JB03223.

Schmidt, J. (1932), *Dana's Togt Omkring Jorden, 1928–1930*, 269 pp., Gyldendal, Copenhagen.

Sdrolias, M., W. R. Roest, and R. D. Müller (2004), An expression of Philippine Sea plate rotation: The Parece Vela and Shikoku basins, *Tectonophysics*, *394*, 69–86, doi:10.1016/j.tecto.2004.07.061.

Sewell, R. B. S. (1934), The John Murray expedition to the Arabian Sea, *Nature*, *134*, 686–690.

Sloan, H., and P. Patriat (1992), Kinematics of the North American-African plate boundary between 28° and 29° N during the last 10 My: Evolution of the axial geometry and spreading rate and direction, *Earth Planet. Sci. Lett.*, *113*, 323–341, doi:10.1016/0012-821X(92)90137-K.

Smewing, J. D., I. L. Abbotts, L. A. Dunne, and D. C. Rex (1991), Formation and emplacement ages of the Masirah ophiolite, Sultanate of Oman, Geology, *19*, 453–456, doi:10.1130/0091-7613(1991)019<0453:FAEAOT>2.3.CO;2.

Solov'ev, V. D., V. A. Zimoglyadov, A. M. Karasik, O. M. Rusakov, and V. N. Yanovskii (1984), Magnetic anomalies over the junction of the Sheba Mid-Ocean Ridge and the Owen fracture zone, *Geophys. J.*, *5*(3), 447–454.

Spencer, S., D. K. Smith, J. R. Cann, J. Lin, and E. McAllister (1997), Structure and stability of non-transform discontinuities on the Mid-Atlantic Ridge between 24°N and 30°N, *Mar. Geophys. Res.*, *19*, 339–362, doi:10.1023/A:1004200411959.

Stampfli, G. M., and G. D. Borel (2002), A plate tectonic model for the Paleozoic and Mesozoic constrained by dynamic plate boundaries and restored synthetic oceanic isochrons, *Earth Planet. Sci. Lett.*, *196*, 17–33, doi:10.1016/S0012-821X(01)00588-X.

Stein, C. A., and J. R. Cochran (1985), The transition between the Sheba ridge and the Owen basin: Rifting of old oceanic lithosphere, *Geophys. J. R. Astron. Soc.*, *81*, 47–74.

Sykes, L. R. (1968), Seismological evidence for transform faults, sea floor spreading, and continental drift, in *History of the Earth's Crust, A Symposium*, edited by R. A. Phinney, pp. 120–150, Princeton Univ. Press, Princeton, N. J.

Sykes, L. R., and M. Landisman (1964), The seismicity of the east Africa, the Gulf of Aden and the Arabia and Red Seas, *Bull. Seismol. Soc. Am.*, *54*, 1927–1940.

Tamsett, D., and R. W. Girdler (1982), Gulf of Aden axial magnetic anomaly and the Curie temperature isotherm, *Nature*, *298*, 149–151, doi:10.1038/298149a0.

Tamsett, D., and R. C. Searle (1988), Structure and development of the midocean ridge plate boundary in the Gulf of Aden: Evidence from Gloria side scan sonar, *J. Geophys. Res.*, *93*, 3157–3178, doi:10.1029/JB093iB04p03157.

Tamsett, D., and R. C. Searle (1990), Structure of the Alula-Fartak fracture zone, Gulf of Aden, *J. Geophys. Res.*, *95*, 1239–1254, doi:10.1029/JB095iB02p01239.

Taylor, B., A. Goodliffe, F. Martinez, and R. Hey (1995), Continental rifting and initial sea-floor spreading in the Woodlark Basin, *Nature*, *374*, 534–537, doi:10.1038/374534a0.

Taylor, B., A. M. Goodliffe, and F. Martinez (1999), How continents break up: Insights from Papua New Guinea, *J. Geophys. Res.*, *104*, 7497–7512, doi:10.1029/1998JB900115.

Tibéri, C., S. Leroy, E. d'Acremont, N. Bellahsen, C. Ebinger, A. Al-Lazki, and A. Pointu (2007), Crustal geometry of the northeastern Gulf of Aden passive margin: Localization of the deformation inferred from receiver function analysis, *Geophys. J. Int.*, *168*, 1247–1260, doi:10.1111/j.1365-246X.2006.03294.x.

Tucholke, B. E., J. Lin, and M. C. Kleinrock (1998), Megamullions and mullion structure defining oceanic metamorphic core complexes on the Mid-Atlantic Ridge, *J. Geophys. Res.*, *103*, 9857–9866, doi:10.1029/98JB00167.

Ukstins, I. A., P. R. Renne, E. Wolfenden, J. Baker, D. Ayalew, and M. Menzies (2002), Matching conjugate volcanic rifted margins: $^{40}Ar/^{39}Ar$ chronostratigraphy of the pre- and syn-rift bimodal flood volcanism in Ethiopia and Yemen, *Earth Planet. Sci. Lett.*, *198*, 289–306, doi:10.1016/S0012-821X(02)00525-3.

Vernant, P., et al. (2004), Present-day crustal deformation and plate kinematics in the Middle East constrained by GPS measurements in Iran and northern Oman, *Geophys. J. Int.*, *157*, 381–398, doi:10.1111/j.1365-246X.2004.02222.x.

Vigny, C., P. Huchon, J. C. Ruegg, K. Khanbari, and L. M. Asfaw (2006), Confirmation of Arabia plate slow motion by new GPS data in Yemen, *J. Geophys. Res.*, *111*, B02402, doi:10.1029/2004JB003229.

Vine, F. J., and D. H. Matthews (1963), Magnetic anomalies over oceanic ridges, *Nature*, *199*, 947–949, doi:10.1038/199947a0.

Vink, G. E. (1982), Continental rifting and the implications for plate tectonics reconstructions, *J. Geophys. Res.*, *87*, 10,677–10,688, doi:10.1029/JB087iB13p10677.

Watchorn, F., G. J. Nichols, and D. W. J. Bosence (1998), Rift-related sedimentation and stratigraphy, southern Yemen (Gulf of Aden), in *Sedimentation and Tectonics of Rift Basins: Red Sea‐ Gulf of Aden*, edited by B. H. Purser and D. W. J. Bosence, pp. 165–191, Chapman and Hall, London.

Wessel, P., and W. H. F. Smith (1991), Free software helps map and display data, *Eos Trans. AGU*, *72*, 441, doi:10.1029/90EO00319.

Whitmarsh, R. B. (1979), The Owen Basin off the south-east margin of Arabia and the evolution of the Owen Fracture Zone, *Geophys. J. R. Astron. Soc.*, *58*, 441–470.

Whitmarsh, R. B., et al. (1974), *Initial Report Deep Sea Drilling Project*, vol. 23, 1180 pp., U. S. Govt. Print. Off., Washington, D. C.

Wiseman, J. D. H., and R. B. S. Sewell (1937), The floor of the Arabian Sea, *Geol. Mag.*, *74*, 219–230, doi:10.1017/S001675680008972X.

Wolfenden, E., C. Ebinger, G. Yirgu, A. Deino, and D. Ayalew (2004), Evolution of the northern Main Ethiopian rift: Birth of a triple junction, *Earth Planet. Sci. Lett.*, *224*, 213–228, doi:10.1016/j.epsl.2004.04.022.

Yatheesh, V., G. C. Hattacharya, and J. Dyment (2009), Early oceanic opening off western India-Pakistan margin: Tha Gop Basin revisited, *Earth Planet. Sci. Lett.*, *198*, doi:10.1016/j.epsl.2009.04.044.

Zeyen, H., F. Volker, V. Wehrle, K. Fuchs, S. V. Sobolev, and R. Altherr (1997), Styles of continental rifting crust-mantle detachement and mantle plume, *Tectonophysics*, *278*, 329–352, doi:10.1016/S0040-1951(97)00111-X.

A. Al-Kathiri, Directorate of Minerals, PO Box 205, PC 211 Salalah, Sultanate of Oman.

L. Audin, IRD, Observatoire Midi-Pyrénées, 14 av. Edouard Belin, F-31400 Toulouse, France.

M.-O. Beslier, Géosciences Azur, UMR 6526, Observatoire Océanologique, CNRS, BP48, F-06235 Villefranche-sur-mer, France.

N. Chamot-Rooke, Laboratoire de Géologie, CNRS UMR 8538, Ecole normale supérieure, 24 rue Lhomond, F-75005 Paris, France.

E. d'Acremont, M. Fournier, P. Huchon, C. Lepvrier, S. Leroy, and C. Petit, iSTeP, UMR 7193, Université Pierre et Marie Curie-Paris 6, UPMC Paris Universitas, CNRS, Case 129, 4 place Jussieu, F-75252 Paris, France. (marc.fournier@upmc.fr)

O. Fabbri, Département de Géosciences, UMR 6249, Université de Franche-Comté, CNRS, 16 route de Gray, F-25030 Besançon, France.

J.-M. Fleury, Total E&P Angola, TTA 208, DEX/TGO, Luanda, Angola.

K. Khanbari, Yemen Remote Sensing and GIS Center, Sana'a University, PO Box 205, PC 211, Sana'a, Yemen.

B. Maillot, Département Géosciences Environnement, Université de Cergy-Pontoise, 5 mail Gay-Lussac, Neuville-sur-Oise, F-95031 Cergy-Pontoise, France.

S. Merkouriev, Marine Geomagnetic Investigation Laboratory, SPbFIZMIRAN, Muchnoy per., 2, Box 188, St. Petersburg 191023, Russia.